1967

The effects of the material properties of copper-tungsten and silver-tungsten composites on the electrical discharge machining wear ratio

Ralph H. Keen
Lehigh University

THE EFFECTS OF THE MATERIAL PROPERTIES

OF COPPER-TUNGSTEN AND SILVER-TUNGSTEN

COMPOSITES ON THE ELECTRICAL DISCHARGE

MACHINING WEAR RATIO

by

Ralph H. Keen

A Thesis

Presented to the Graduate Faculty

of Lehigh University

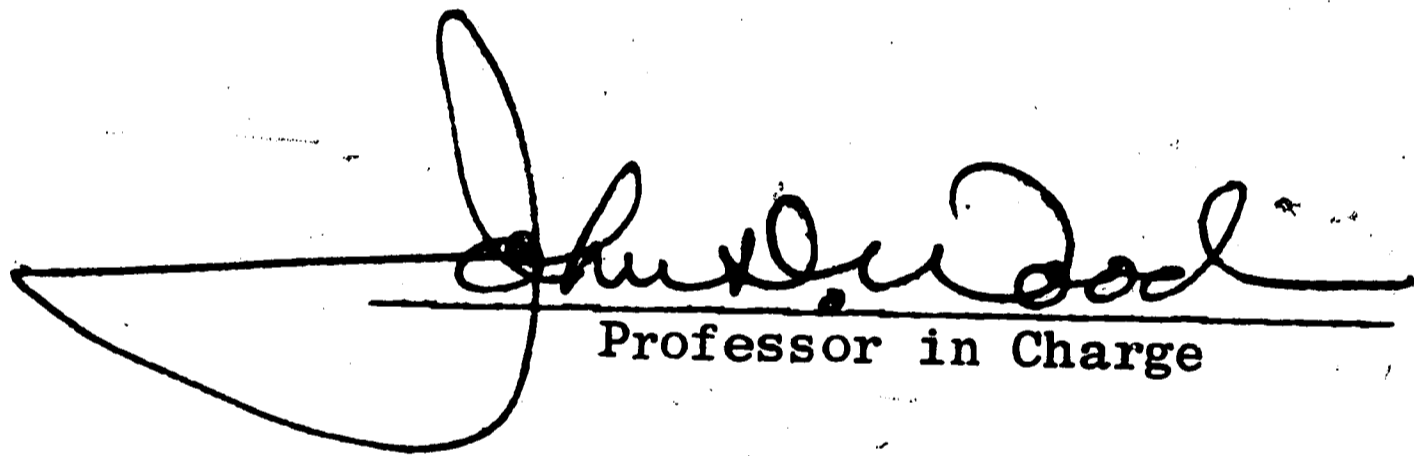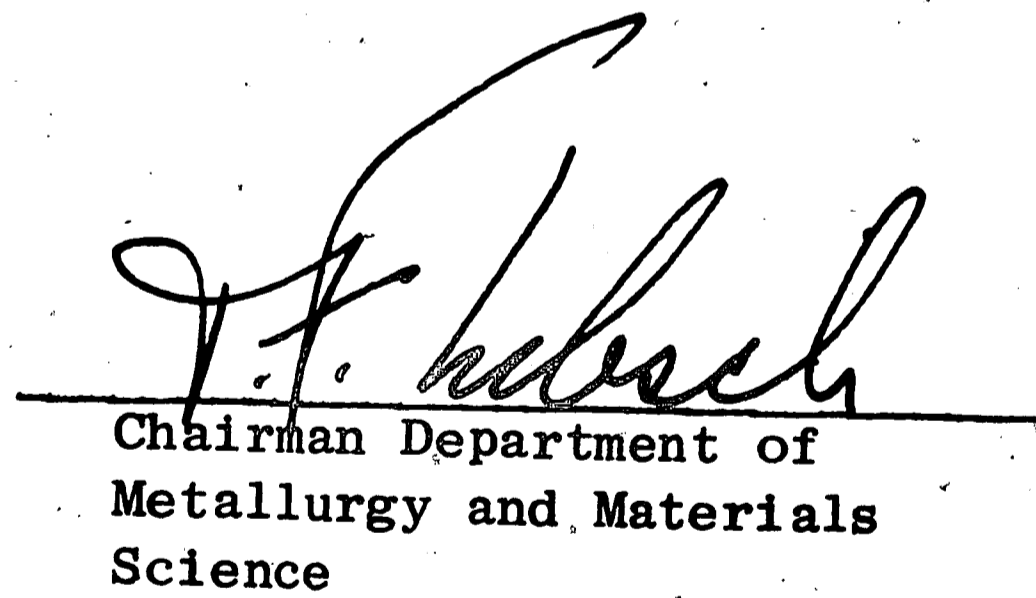in Candidacy for the Degree of

Master of Science

Lehigh University

1967

CERTIFICATE OF APPROVAL

This thesis is accepted and approved in partial fulfillment of
the requirements for the degree of Master of Science.

May 24, 1967
Date

Professor in Charge

Chairman Department of
Metallurgy and Materials
Science

ACKNOWLEDGMENTS

TABLE OF CONTENTS

v

LIST OF FIGURES

viii

LIST OF TABLES

ABSTRACT

Eight compositions of copper-tungsten composites, eight compositions of silver-tungsten composites, as well as copper, silver and tungsten tool electrodes were used to machine copper and molybdenum workpieces. The objective of the investigation was to define the wear ratio of these materials in terms of cohesive energy and electrical conductivity.

The copper-tungsten and silver-tungsten materials gave wear ratios consistently higher than the wear ratio of tungsten alone. This increase in the wear ratio cannot be explained solely in terms of cohesive energy and electrical conductivity. A possible explanation, based on the capillarity of the tungsten matrix trapping and forcing the infiltrant to vaporize, is proposed. Also the possibility of interaction between the boiling point of the infiltrant and the discharge channel pressure is discussed.

INTRODUCTION

The Electrical Discharge Machining Process

Electrical discharge machining (EDM), a process of material removal by electric spark erosion, was developed in Russia during and immediately after World War II[1]. The process was gradually adopted by industry outside of Russia and is now a well established material removal process, especially in the die sinking industry.

The basic attribute of electric spark erosion is that no known material can withstand the electro-thermal release of energy caused by a spark discharge between two closely spaced electrodes[2]. The amount of material removed by each spark is minute, but successive application of sparks at a high frequency will result in significant material removal. Some of the factors affecting the amount of material removed are:

1. The intensity and the duration of the spark.

2. The polarity of the electrode.

3. The intrinsic material properties of the electrodes.

4. The dielectric medium in which the spark breakdown occurs.

Conditions common to most EDM processes are; (1) the polarity of the tool electrode is negative and the workpiece electrode is positive, (2) the dielectric is liquid (usually similar to kerosene). These conditions generally cause more material to be removed from the workpiece than from the tool. The wear between the tool and the workpiece is commonly measured by the volumetric wear ratio[3],

where

Wear Ratio (WR) = $\dfrac{\text{volume of workpiece material removed}}{\text{volume of tool material removed}}$.

Most of the literature on the wear ratio in EDM is concerned with the effects of spark intensity and spark duration[4]. As a result, the effects of the spark variables is relatively well defined. However, the effect of material properties on the wear ratio is not well defined and is still subject to controversy.

Review of the Literature

Literature on EDM is beset with a lack of common agreement in regard to the theory. A good review of EDM theories is given by Hill[5].

In recent years most investigators have come to generally accept that EDM is basically a thermal process[6]. However, mechanical forces cannot be overlooked. Longfellow[7] found that low-strength, brittle materials such as antimony, bismuth and tellurium exhibited material removal by fracture.

In a general review of the theoretical aspect of erosion by a thermal process, Nekrashevich and Bakuto[6] state that a thermal theory should be based on the equation

$$\partial T/\partial t = \frac{1}{c\,\delta}\left[\text{div}\,(\,\lambda\,\text{grad}\,T)\,+\,\eta\,\rho\,(T)j^2\right]$$

Where:

   c = heat capacity of the material

   δ = density of the material

λ = thermal conductivity of the material

ρ = electrical resistivity of the material

j = current density of the spark

η = thermal equivalent of mechanical work

t = time

T = temperature

Although this equation is difficult, if not impossible, to solve in a general way, approximate solutions have been obtained by making a large number of simplifying assumptions. The most notable solution, due to A. S. Zingerman of the Leningrad Cine-Engineers Institute, is reviewed by Berghausen et al[8]. Zingerman's basic assumption is that the Joule heating effect is not significant, thus, the second term in the above equation can be dropped. With this simplification, the above equation can be reduced to:

$$\partial T/\partial t = \lambda(\nabla^2 T)/c\delta.$$

Then by assuming that; (1) c, λ and δ are constants, (2) the spark can be represented by a plane, circular heat source, and (3) the electrode can be represented by an infinite metallic solid; Zingerman derived an expression for the temperature at any depth in the material. On the assumption that all the material is removed in the molten state and knowing the crater shape (conical, parabolic, etc.), the amount of material eroded per spark can be estimated.

The details of Zingerman's derivation are too involved to develop here, but the most often cited result of his work is

$$F = 1.13 \, (\delta \, c \, \lambda)^{\frac{1}{2}} (T_m + q/2c);$$

where F is a figure of merit expressing the resistance of the material to EDM erosion, T_m is the melting point of the material, q is the latent heat of fusion of the material, and the remaining terms (δ, c, and λ) are as previously defined. Later, Zingerman[9] extended his theory to include material eroded by both vaporization and melting. However, this extension lends itself to verification by varying the spark intensity and duration rather than by varying the material properties of the electrodes, thus, it is of little value in this investigation.

Using the energy balance approach, Jones[10] derived the following relation for the material removed per spark.

$$v = \left[W - b\theta^4 - qk(\theta - T) \right] / \delta \left[c \, (\theta - T) + 2i\theta/M \right]$$

where v is the volume of material removed

W = energy of the spark

θ = boiling point of the material

T = initial temperature of the material

δ = density of the material

M = molecular weight of the material

k = thermal conductivity of the material

c = heat capacity of the material

b and g are constants determined by the area of the
spark, and the emissivity of the material.

The basic limiting assumptions in Jones's derivation are that: (1) the anode and cathode are of the same material and (2) the duration of the pulse should exceed 10^{-4} seconds. Also his derivation is an extension of electric contact erosion theory and the direct application of this to EDM is subject to question. Other derivations based on themodynamic considerations are given in the Russian literature and a good review is found in Nekrashervich's paper[6].

Experimental work relating the material properties of the electrodes to the wear ratio supports the thermal process theory in general. Williams and Smith[11] machined with pure metals and metal alloys using short, low power sparks and a kerosene dielectric. They concluded that cathode (tool) erosion depends in a general way upon the melting point of the material.

Price[12] machined with tungsten, copper, palladium, and five copper-palladium alloys using short pulses and a dielectric similar to kerosene. Price concluded that prior deformation and the order-disorder transformation in the Cu-Pd system had little effect on the wear ratio. In addition he found that wear ratio was dependent on the cohesive energy of the anode (work piece) in an inverse manner.

Longfellow[7] machined with 35 elements as tools and with four elements as workpieces using short pulses and dielectric similar to kerosene. He found that erosion by mechanical means to be minor and

limited to low-strength, brittle materials. Longfellow concluded that those physical properties of an electrode material which govern the wear ratio in EDM are:

(a) The cohesive energy of the tool and the cohesive energy of the workpiece, related in a general manner, by

$$\text{Wear Ratio} = A \left[\frac{\text{Cohesive energy of the tool}}{\text{Cohesive energy of the workpiece}} \right]^B ,$$

where A and B are constants dependent on the workpiece machined.

(b) The electrical conductivity of the electrode materials.

(c) The mechanical strength and toughness of the electrode materials.

(d) The ratio of the boiling point to melting point of the electrode materials.

The literature cited presents evidence that the thermal and electrical properties are significant material properties affecting wear ratio. However, there is still much room for definitive investigations relating the wear ratio to these properties. The purpose of this investigation is to attempt to define the effects of the cohesive energy and the electrical conductivity of the tool (cathode) on the wear ratio.

Desired Experimental Criteria

Much of the experimental effort in EDM has been difficult to interpret as a result of the inability to control the parameters involved in the process. It was believed that to produce reliable,

definitive results the following conditions should be observed.

1. The intensity of the spark, which is determined primarily
   by the current, should be constant for each pulse.

2. The total number of machining pulses should be kept to a
   minimum value to prevent cavity depth effects (i.e., residue
   collecting in the gap due to poor dielectric circulation).

3. The range of materials to be tested should have a significant
   and predictable variation of the parameters to be investi-
   gated.

The first requirement can be satisfied by refinement and sophis-
tication of the equipment used. It was felt that the last require-
ment could be met by selecting various compositions of silver-tungsten
and copper-tungsten binary composites for tools.

EXPERIMENTAL PROCEDURE

Tool Materials

Various compositions of silver-tungsten and copper-tungsten composites, which consist of a tungsten matrix infiltrated with copper or silver, were chosen as tool materials. Fabrication in this manner is possible over a range of about 0.20 to 0.65 volume fraction of infiltrant. These materials were selected for the following reasons:

1. The conductivity (electrical and thermal) vary as near linear functions of the volume fraction of infiltrant.

2. It was assumed that the effective cohesive energy* of the infiltrated materials could be varied linearly as a function of the volume fraction of infiltrant.

3. A complete, definitive investigation of the EDM wear ratios for silver-tungsten and copper-tungsten infiltrated material has not been reported in the literature.

Also silver, copper, and tungsten were used to provide end point wear ratio data for each composition range.

The effective cohesive energy and the electrical conductivity in a given composite system cannot be varied independently, as both are dependent on the volume fraction of infiltrant. Therefore, using the two systems, silver-tungsten and copper-tungsten, allows

---

*The term "effective cohesive energy" means the energy required to sublimate the material at $298^{\circ}K$. It is assumed that the materials sublimate without interaction.

one to select; (1) compositions with equivalent effective cohesive energies or (2) compositions with equivalent electrical conductivities. The properties of the composite materials are listed in Table I, and the properties of the elemental materials are listed in Table II.

Workpiece Materials

Copper and molybdenum were selected as workpiece materials for the following reasons:

1. They are both considered relatively good conductors, but there is a significant difference in their electrical conductivity.

2. They both have sufficient mechanical strength to minimize material removal by mechanical means (i.e., by fracturing from the mechanical forces generated by the spark).

3. Their cohesive energies are significantly different.

4. They serve as a continuity link between the investigation and Longfellow's[7] investigation, since Longfellow used copper and molybdenum workpieces (among others).

The properties of these materials are also listed in Table II.

Material Specifications

The tungsten, copper, and silver used in the infiltrated tool material were manufactured by the Mallory Metallurgical Company's standard procedure for these materials. Previous metallurgical history of this material such as particle size distribution of the tungsten powder, compaction methods, sintering times, and infiltra-

tion methods were not given. Tool samples with a 0.125 inch square cross-section and 1.25 inches long were cut from the infiltrated material supplied.

The tungsten, copper, and silver tools used to obtain end point wear ratios were of 99.5% purity. These tools were 0.125 in. in diameter and approximately 1.25 in. long. The molybdenum and copper workpieces were of 99.5% purity. The workpieces were 0.25 in. in diameter and 0.25 in. long.

Description of the EDM Equipment

The power supply used in this investigation was a modified resistance-capacitance (RC) circuit. The primary modification was the addition of an electronic switch to discharge the capacitor into the electrode gap. The electronic switch consisted of a silicon controlled rectifier (SCR), triggered through a pulse transformer from a (Hewlette Packard, Model 214A) pulse generator. The triggering pulse was approximately four microseconds in duration with a repetition frequency of 500 cycles/second. The purpose of this modification was to allow the voltage on the capacitor to recharge to the same voltage prior to each discharge.

The capacitor used in this circuit was specifically designed for pulse applications. The capacitor was recharged after each spark through a 900 ohm resistor from a 325 v.d.c., 0.5 ampere electronically regulated power supply (Lambda, model C-282M).

To monitor and measure the discharge current, a wide-band coaxial type shunt was used. The design of the shunt was similar

to Park's[13], and has frequency response of d.c. to 2 megacycles/ second. This shunt was made a permanent part of the discharge circuitry. The shunt, capacitor, and SCR switch were mounted in the dielectric tank adjacent to the machining gap. Connections were made with short, heavy copper leads to reduce external resistance and inductance.

A schematic of the SCR switch, capacitor, and current shunt combined with a block diagram of the d.c. power supply and pulse generator is shown in Figure 1. The discharge current and gap voltage are shown in Figure 2 for a typical machining pulse. Note the peak current is approximately 200 amperes and has the character- istic shape of an overdamped circuit (i.e., the current is uni- directional) which prevents the adverse polarity reversal effects mentioned by Price[12].

The primary disadvantage of the modified RC circuit is the difficulty of obtaining an average gap voltage sufficient to drive existing sevo systems. To illustrate the problem consider a breakdown-recharge cycle. The breakdown of the gap is of approx- imately 5 microseconds duration with an average voltage of approx- imately 20 volts. On the other hand the recharge period is approx- imately 1995 microseconds and the gap voltage is zero. Thus the average gap voltage is 0.05 volts which is not sufficient for most servo systems. To solve this problem a "sample and hold" technique was used.

The "sample and hold" technique consisted of connecting a capacitor to the gap with an electronic (transistor) switch in synchonous with, and during the first 3 microseconds of the gap breakdown. This allows the capacitor to charge to the average voltage of the gap during the machining pulse. Then the capacitor is disconnected from the gap and this voltage is "held" until the next machining pulse. The average voltage derived by this method (about 20 volts) was quite sufficient to drive the servo used.

The servo amplifier, the servo drive motor, and the quill were part of an Agiepuls EDM machine (manufactured by the Agie Company, Losone-Locarno, Switzerland). The Agiepuls servo amplifier was modified to use the "sample and hold" voltage as a gap signal which, in turn, operated the servo drive motor and maintained a suitable electrode spacing for spark breakdown.

Measurement of Wear Ratio

The wear ratio tests were performed by machining a blind, square hole into the workpiece. The wear ratio was calculated using the following formula,

$$WR = \frac{(\text{weight loss of workpiece})(\text{tool density})}{(\text{weight loss of tool})(\text{workpiece density})}.$$

Prior to each machining test the mating surfaces of the tool and workpiece were polished with fine "0" grit polishing paper. This was found to be sufficient to produce good starting characteristics.

The weight loss of the tools and the workpieces were determined by weighing on a Mettler (Model 5B) analytical balance, capable of $\pm$ 0.0001 gram accuracy. The tools and workpieces were cleaned in an ultrasonic bath of denatured alcohol prior to each weighing. The Mettler analytical balance was also used for the density measurements which were determined by the weight-in-air, weight-in-liquid method. The liquid used for the density measurements was carbon tetrachloride (CCl_4), chosen for its good wetting characteristics and ease of making corrections in its density resulting from changes in temperature. Corrections were not made for the bouyancy of the air.

The dielectric medium for the machining test was a hydracarbon, Mobil Solvasol No. 6 which was recirculated through a 1 micron filter. Each machining test was conducted in static fluid within a temperature range of 24-28°C.

Electrical Conductivity Measurements

The electrical conductivity of the tool materials was measured by the voltmeter-ammeter method. A block diagram of the conductivity test equipment is shown in Figure 3. The tests were performed by establishing a 10 $\pm$ 0.1 ampere current through the tool sample. The voltage drop between two knife edges, spaced 2 cm. apart, was measured and the sample resistance (R) between the knife edges was calculated from Ohm's law. The average cross-sectional area (A) of sample was measured and the electrical conductivity (σ) was

calculated from

$$\sigma = 2/RA \ (ohm-cm.)^{-1}.$$

It is expected that the conductivity measurements will be slightly lower than calculated from the linear model, as this model does not take into account porosity and possible microstructure effects in the composite materials.

Metallographic Measurements

The volume fraction of infiltrant, the open porosity, and the number of infiltrant-matrix intercepts per millimeter were determined by quantitative metallographic techniques[14]. The volume fraction of infiltrant and the open porosity were found by using the point counting techniques and the intercepts per millimeter was found by counting the number of infiltrant-matrix boundaries intersecting a line of known length.

The point counting was accomplished by using a 121 point square grid, positioned at random on the unetched, polished surface of the material sample. The intercept count was obtained by counting the intersections along one edge of the grid. Ten, randomly positioned, point counts and intercept counts were made on each sample (i.e., each composition) to reduce the statistical variation of the measurements to a reasonable value. The ten count figure is based on a "rule of thumb" given by Underwood[15].

The volume of infiltrant (V_i) was determined from the point count by using the relation

$$V_i = \frac{\text{Number of points falling in infiltrant phase}}{\text{Total number of points}}$$

It was felt that two other parameters, the interfacial area per unit volume (S_V) and the mean free distance (MFD) between the infiltrant "particles", might be related to the wear ratio test results. The interfacial wear per unit volume was found using the relation

$$S_V = 2 \, N_L,$$

where N_L is the number of interfaces per unit length intersected by a random line. The mean free distance between the infiltrant "particles" was determined by[16]

$$MFD = \frac{1 - V_1}{N_L} \, .$$

RESULTS AND DISCUSSION

Machining Characteristics

The average value of the wear ratios obtained for eight compositions of copper-tungsten, eight compositions of silver-tungsten, pure copper, pure silver, and pure tungsten are listed in Table III and the results of the individual tests are listed in Table IV. All the materials used had excellent general machining characteristics in regard to shorting and machining efficiency.*

The characteristics of the spark breakdown were typical of previous descriptions in the literature. That is, the discharge was accompanied by sparks shooting from the gap, explosive sounds, bubbles of gas, and a carbonaceous cloud of debris was ejected into the dielectric. Several samples of the contents of the tank were filtered and examined with a microscope for clues as to how the material was removed. There was no evidence that material was removed by other than thermal means (i.e., by vaporization and melting as opposed to mechanical removal).

Results of Tests

In order to get at least an indication of the expected results, Longfellow's data (Table V) were analyzed using the cohesive energy and electrical conductivity as prediction criterion. Multiple regression techniques were used to arrive at an emperical mathematical model to describe Longfellow's results. From his results it

---

*The term "machining efficiency" is defined as the ratio of the number of spark discharges to the number of pulses applied to the machining electrodes.

appeared that the electrical conductivity only affected the wear ratio appreciably when the conductivity was greater than 0.125 $(\text{microhm-cm})^{-1}$. On this basis copper, gold, silver, cadmium, zinc, cobolt, nickel, molybdenum, and tungsten were selected for analysis. Using the molybdenum workpiece data, these nine elements were found to fit the following formula with a correlation coefficient of 0.994:

$$WR_{Mo} = 0.0085 \ ((\sigma + 0.2)/0.2)^{2.99} \exp(3.125 L_T / L_W).$$

When using copper workpiece data, the following formula was fitted with a correlation coefficient of 0.997:

$$WR_{Cu} = 0.031 \ ((\sigma + 0.2)/0.2)^{2.38} \exp(1.783 L_T / L_W).$$

For both of the above formulas:

σ = electrical conductivity of the tool material

L_T = cohesive energy of the tool material

L_W = cohesive energy of the workpiece material

It should be noted that _neither_ of the above _formula_ is intended to represent a general relation between the wear ratio and the material properties. They are intended only to be used as an indicator of the expected results for this investigation. Since the composite materials for this investigation have an electrical conductivity greater than 0.125 $(\text{microhm-cm})^{-1}$, and since the machining conditions for this investigation were similar to Longfellow's, it was felt that these formulas would be indicative of the expected results.

The predicted results* and the actual results are presented graphically in Figures 4-7. It is evident from the graphs that the wear ratios for the composite, infiltrated materials are considerably higher than predicted. Thus, it was felt that the results could not be totally explained on the basis of cohesive energy and electrical conductivity alone.

A Possible Explanation

To develop an alternative explanation, a brief review of the theory of the mechanism of EDM material removal should be considered. Several theories have been developed regarding this mechanism and a review of them is given by Hill[5]. There is evidence to indicate[9], and there is general agreement, that material leaves the spark gap by both vaporization and liquid ejection. However, nothing can be stated quantitatively about the relative amounts of the material removed in the vapor or the liquid phase.

The relative amounts of the material removed by vaporization and by melting appear to depend on many factors such as spark intensity and duration, melting point/boiling point ratio, surface tension and cohesive energy to name a few. However, for infiltrated composite materials it appears that additional factors should be considered.

In an experimental study on liquid phase sintering; Naidich,

---

*The "predicted results" were calculated from the emperical wear ratio formula assuming that both effective cohesive energy and electrical conductivity were linear, ideal functions of the volume fraction of the infiltrant material.

Lavrinenko, and Eremenko investigated the forces caused by capillary phenomena of the liquid phase[17]. For a porous tungsten matrice infiltrated with either copper or silver they found, using dilatometry techniques, that the composites exhibited shrinkage when exposed to temperatures above the melting point of the infiltrant. This was explained by the capillary forces arising from the wetting of the matrix by the liquid infiltrant. Evidence was presented showing that the wetting angle of both copper and silver on tungsten decreased with increasing temperature. Also it can be shown that the capillary force is inversely related to the wetting angle. They proposed that as the temperature was increased, the capillary forces increased, causing the matrix to shrink. This suggests that capillary phenomena can result in strong forces of attraction between the infiltrant and the matrix.

In a discussion on electric contacts, Meyer[18] pointed out that tungsten or molybdenum skeletons infiltrated with a high conductivity material, such as copper or silver, make good electrical contacts for heavy duty applications. The reason stated for this was that the refractory skeleton retained the molten, conductive metal which would otherwise be blown away by the electrical arc.

In the literature on vapor cooled rocket engine nozzles, Matt and Warga made the following observation[19]. When infiltrating a porous tungsten matrix with silver, they had difficulty keeping the silver in the matrix when the pore size was large. In general, they found that the difficulty in keeping the silver in the matrix

increased as the infiltration temperature was increased. This was attributed to the increase in fluidity of the infiltrant at the higher temperatures.

On the basis of the above cited literature, the author proposes the following mechanism for composite materials when the boiling point of the infiltrant is less than the melting point of the matrix. The small pores* in the matrix give rise to a capillary action effect. Thus, if the pore size is sufficiently small it would be difficult to remove the infiltrant material in the molten state and the infiltrant would be forced to vaporize. The effect of this would be to increase the energy required to remove a given volume of material. Again, this mechanism would only be valid when the melting point of the matrix is above the boiling point of the infiltrant. If the boiling point of the infiltrant is above the melting point of the matrix, then both materials could be removed by melting and the effect would be lost. Also, since the capillary force in a pore diminishes as the pore size increases, one would expect this effect to be sensitive to the pore size and pore size distribution. If the pore size exceeds some critical value, infiltrant is removed in the liquid state and the effect is lost because the infiltrant is not forced to vaporize.

This proposed material removal mechanism for composite materials

---

*The term "pore" in this section refers to the pre-infiltrated porosity of the tungsten matrix which retains the infiltrant.

correlates well, at least in a quantitative manner, with the observed microstructures of the tool materials. It is expected that as the volume fraction of infiltrant is increased, the amount of energy per unit volume to remove the material will increase proportionately since most of the infiltrant is forced to vaporize. This proportionate increase will continue until a critical pore size is reached (it is expected, and generally observed, that the average pore size will increase as the volume fraction of infiltrant is increased) after which, the fraction of the infiltrant removed in the vapor state begins to decrease. This causes the amount of energy per unit volume required to remove the material to decrease as the average pore size of the matrix continues to increase.

Analysis of Metallographic Data

The slight relief resulting from the different polishing rates of the hard matrix and the soft infiltrant, when using standard metallographic techniques, was usually sufficient to clearly distinguish between the two phases. The volume fraction of voids, resulting from the pores which failed to infiltrate, of the composite samples was obtained by point counting techniques (Table I)[14]. However, it should be mentioned that the void size variation in some of the materials was greater than two orders of magnitude. This made point counting somewhat difficult and, as a result, probably contributed a significant amount of experimental error.

A qualitative examination of the tool material with respect to pore size supported the mechanism of material removal suggested in

the previous section. For the 20% Ag-80%W tool (Figure 8) the pores are small and relatively well defined. However, a look at the 30% Ag-70%W tool (Figure 9) and the 41% Ag-59%W tool (Figure 10) reveals that the pores are larger and less well defined. Continuing to the 50% Ag-50%W tool (Figure 11) the pores are not really defined, but rather, the silver appears as a massive phase dotted with islands of tungsten. The microstructure of Cu-W materials have in general, the same appearance. The following observations were made after metallographic examinations of the tool materials.

1. The pores in the tungsten matrix for materials containing less than 30% infiltrant were relatively well defined. This caused the infiltrant to be removed completely, or nearly completely, in the vapor state. Removal of the infiltrant by vaporization caused an increase in the average energy required to remove a given volume of material, thus, causing a proportionate increase in the wear ratio.

2. For materials with greater than 30% infiltrant, the pore definition diminishes as the volume fraction of infiltrant is increased. This allows removal of infiltrant in a liquid state instead of forcing it to vaporize. Thus, the average energy required to remove a given volume of the material would decrease, causing a proportionate decrease in the wear ratio.

The above observations support the machining test data for the silver-tungsten composite systems (Figures 4 and 5) in a qualitative sense. However, the test data for the copper-tungsten system (Figures 6 and 7) shows a "leveling off" when the volume fraction of infiltrant exceeds 30%. A possible explanation of this effect was noted from examination of the cross-section of the machined surfaces. It was noted that when the infiltrant exceeded 30% for the copper-tungsten materials, a thin, fairly continuous layer of tungsten tended to form on the machined surface (Figure 12). This layer was not noted for comparable silver-tungsten materials (Figure 13). There is no immediate and obvious explanation for this effect, but it is possible that this tungsten layer "traps" the copper infiltrant and forces a larger proportion of the infiltrant to be removed by vaporization.

The volume fraction of infiltrant determined by point counting (Table I) was consistently below the nominal volume fraction quoted by the Mallory Metallurgical Company. This was believed to be due to the etching effects caused by the hardness differential between the infiltrant and the matrix. Underwood[20] states that if this occurs, "a twofold increase in apparent particle size could easily result." Thus, the nominal volume fraction of infiltrant was felt to be a more accurate measure and, as a result, it is used in calculations and graphical data presentations.

There was no apparent relation between the wear ratio and the interfacial area per unit volume (Table I). On the other hand,

it appears that a possible relation may exist between the wear
ratio and the mean free distance of the infiltrant "particles"
(Figures 14 and 15). The extensive metallographic techniques nec-
essary to clarify this relation is beyond the scope of this in-
vestigation[21].

The Role of Vapor Pressure

A somewhat analogous application of infiltrated materials
is found in the literature on vapor cooled, rocket engine nozzles[19,22].
As pointed out by Matt and Warga[19], the amount of heat absorbed to
convert copper from a solid at $20^{\circ}C$ to a vapor at its boiling point
is 13,300 cal./cm^3 as compared to 7,700 cal./cm^3 for silver. This
leads one to expect that copper infiltrated materials would yield
significantly higher wear ratios than the silver infiltrated materials.
However, in direct contradiction to expectations, the opposite is
observed. According to Matt and Warga, although they offer no
explanation, silver infiltrant in rocket nozzles produces better
results than copper infiltrant. As a possible explanation, Resnick
et al[22] proposed that the results would be as expected if the
material was removed at atmospheric pressure. However, in rocket
nozzles the pressure has been estimated to be at least 30 atmos-
pheres. Resnick points out that at 30 atmospheres, the extrapo-
lated vapor pressure data indicates that the boiling point of
copper would be about $3700^{\circ}C$. This is above the melting point of
tungsten, thus, both materials could then be removed by melting.

It is reasonable to expect, and there is supporting evidence[23], that pressures of this magnitude exist in the discharge column of the spark in EDM. Therefore, a possible explanation for the behavior of the copper-tungsten is that the pressure in the discharge channel forces the boiling point of the copper above the melting point of the tungsten matrix. An extrapolation of the vapor pressure data for silver and copper (Figure 16) gives pressures of approximately 60 and 15 atmospheres respectively to raise the boiling point of the infiltrant to the melting point of the tungsten. Therefore, it appears that if the pressure in the discharge exceeds 15 atmospheres, at least for some portion of the discharge period, the "vaporization effect" would be lost, or at least diminished, for copper. Proof of this explanation suffers from the inability to measure or estimate the pressure in the discharge channel.

SUMMARY

The data clearly shows an increase in the EDM wear ratio, relative to the wear ratio of pure tungsten, for porous tungsten compacks infiltrated with copper or silver. This increase in the EDM wear ratio cannot be explained solely in terms of the cohesive energy and the electrical conductivity of the composite material.

A proposed explanation is based on the capillary action between the lower melting point infiltrant and the porous tungsten matrix. The infiltrant is trapped in the tungsten matrix and is forced to leave the material in the vapor state. Thereby, the energy per unit volume to remove the material is increased, resulting in a wear ratio increase.

It was observed that the silver-tungsten composites produced higher wear ratios than the copper-tungsten. This was contrary to the expected results since copper has the higher volumetric heat of vaporization. A possible explanation is that the pressure in the discharge channel forces the boiling point of the copper above the melting point of the tungsten matrix. Under these conditions the copper can be removed in the molten state rather than being forced to vaporize, reducing the required energy per unit volume to re-move the material, hence, giving lower than expected wear ratios.
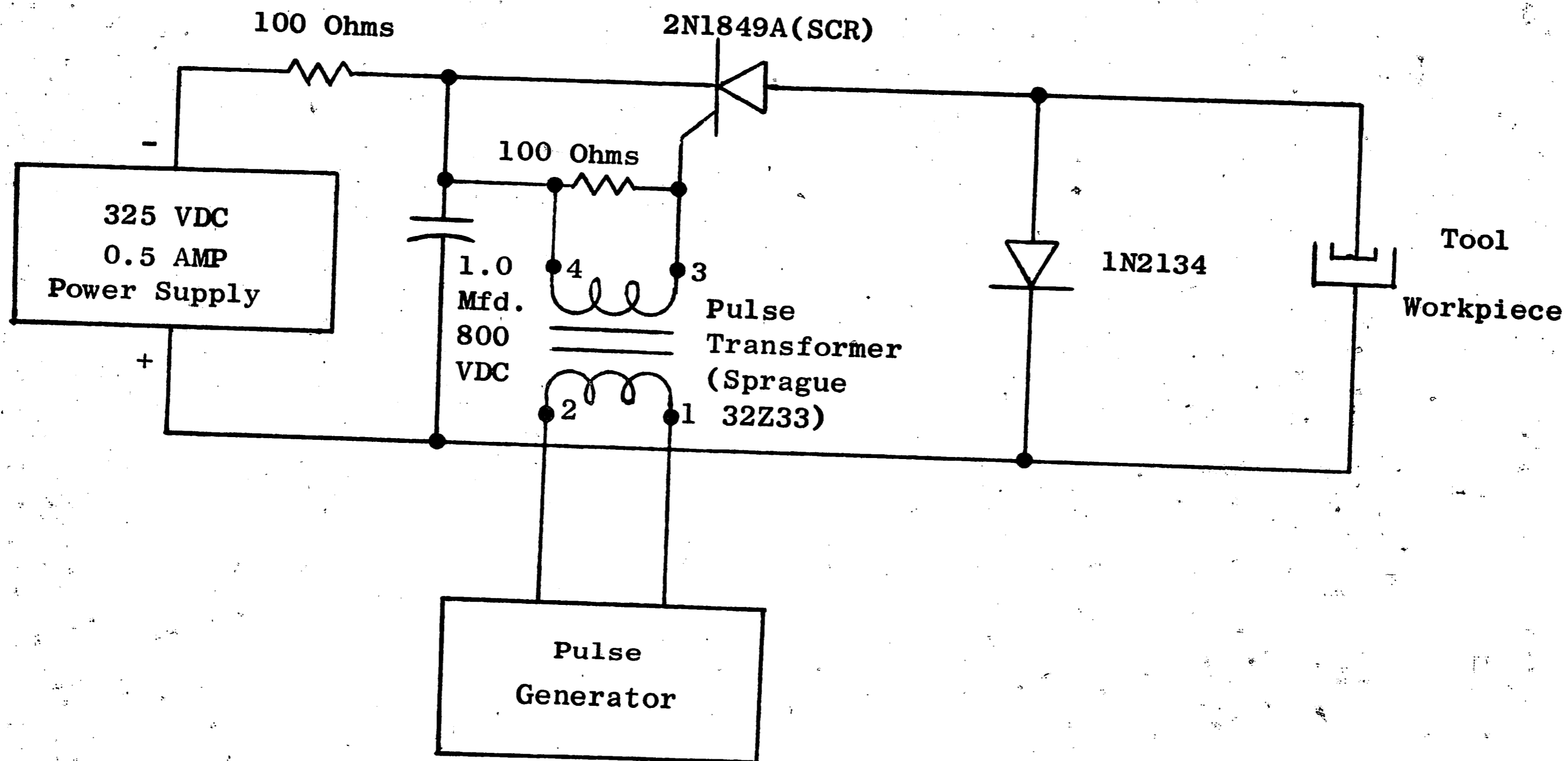
FIGURE 1. Schematic - Block Diagram of EDM Power
Supply Used in This Investigation

A
↑
O-
↓
V
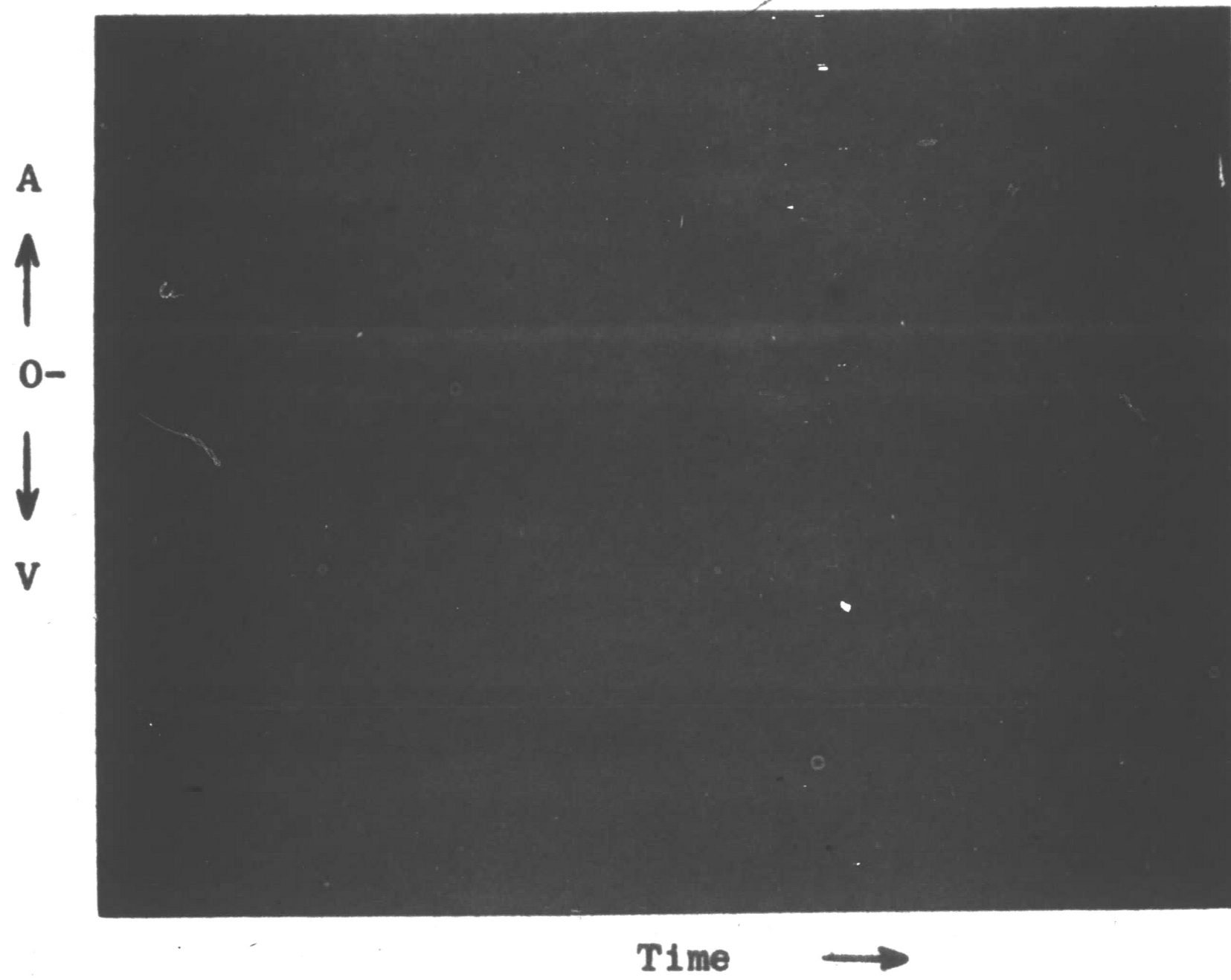
Time ⟶

    Top Trace - Discharge Current, 100 amperes/major
             division
    Bottom Trace - Discharge Gap Voltage, -10 volts/
             major division
    Time Base - 1 microsecond/major division

FIGURE 2. Typical Oscilloscope Traces of the Discharge
Current and Gap Voltage Waveforms

1 Ohm Resistor

Power Supply

Ammeter

Sample of Tool Material

Knife Edges

2 cm.

Voltmeter
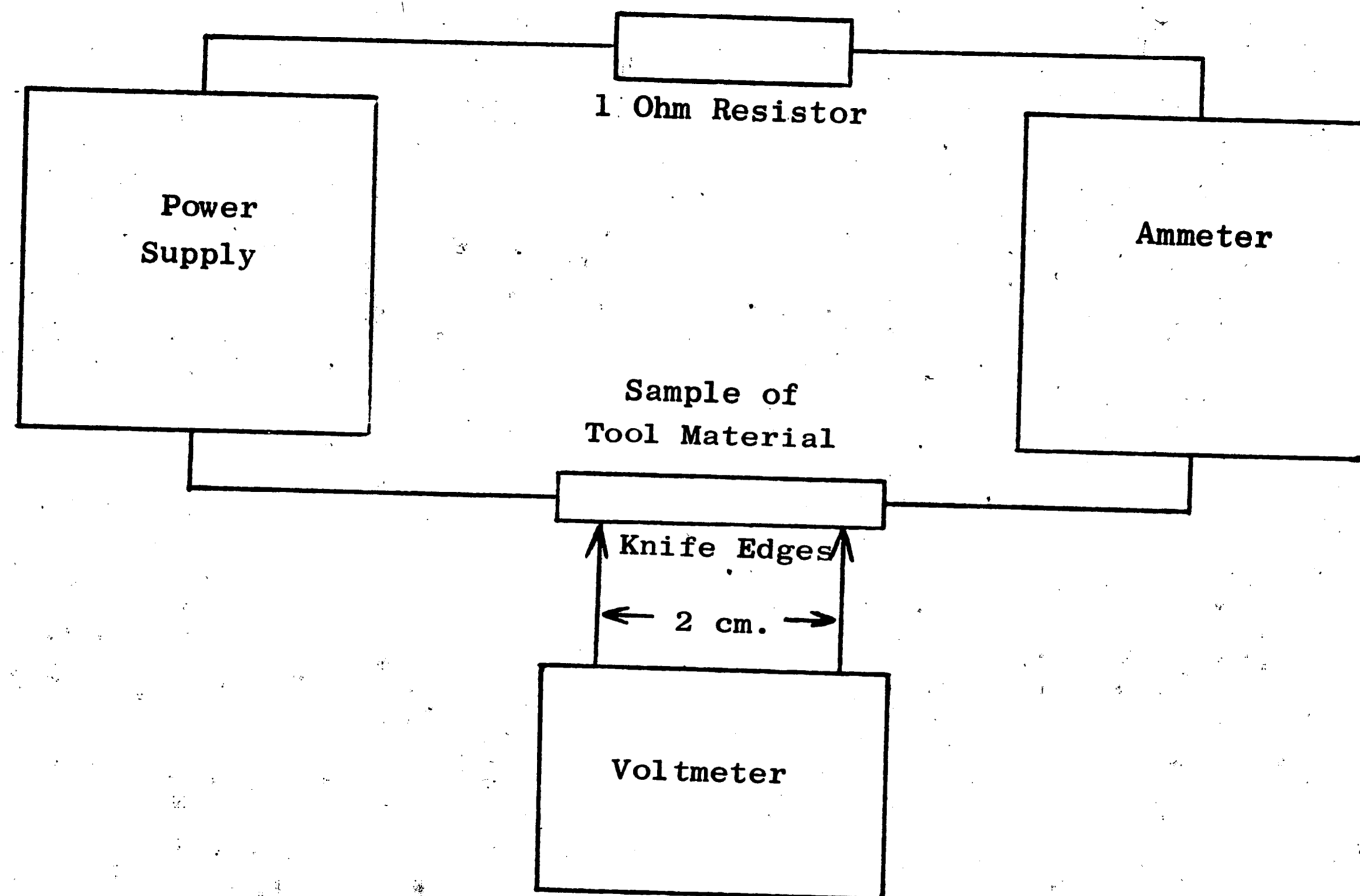
FIGURE 3.   Block Diagram of Conductivity Measurement Test Set
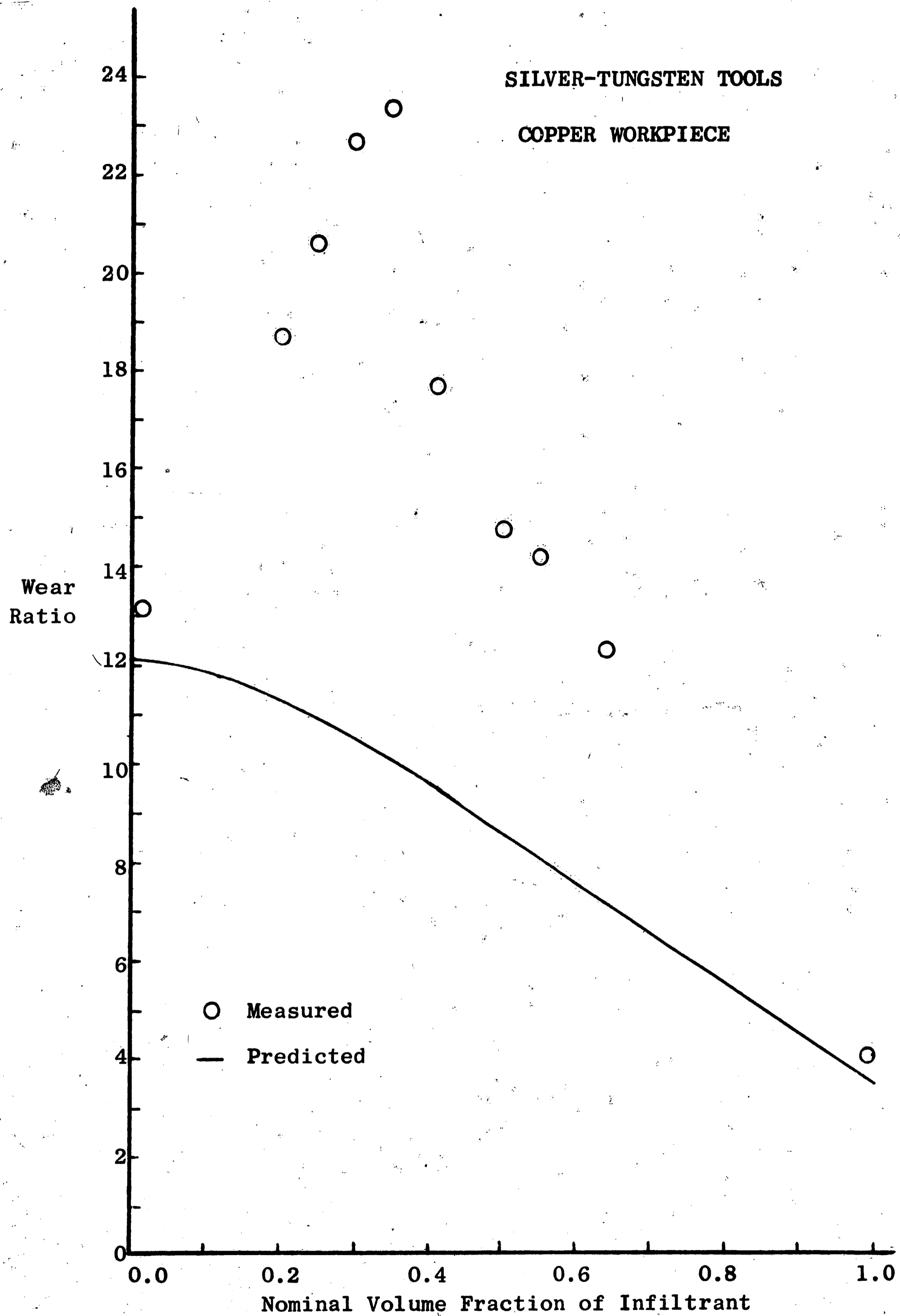
FIGURE 4. Volumetric Wear Ratio Versus Volume Fraction of
Silver Infiltrant (Silver-Tungsten Composite
Tools, Copper Workpiece)
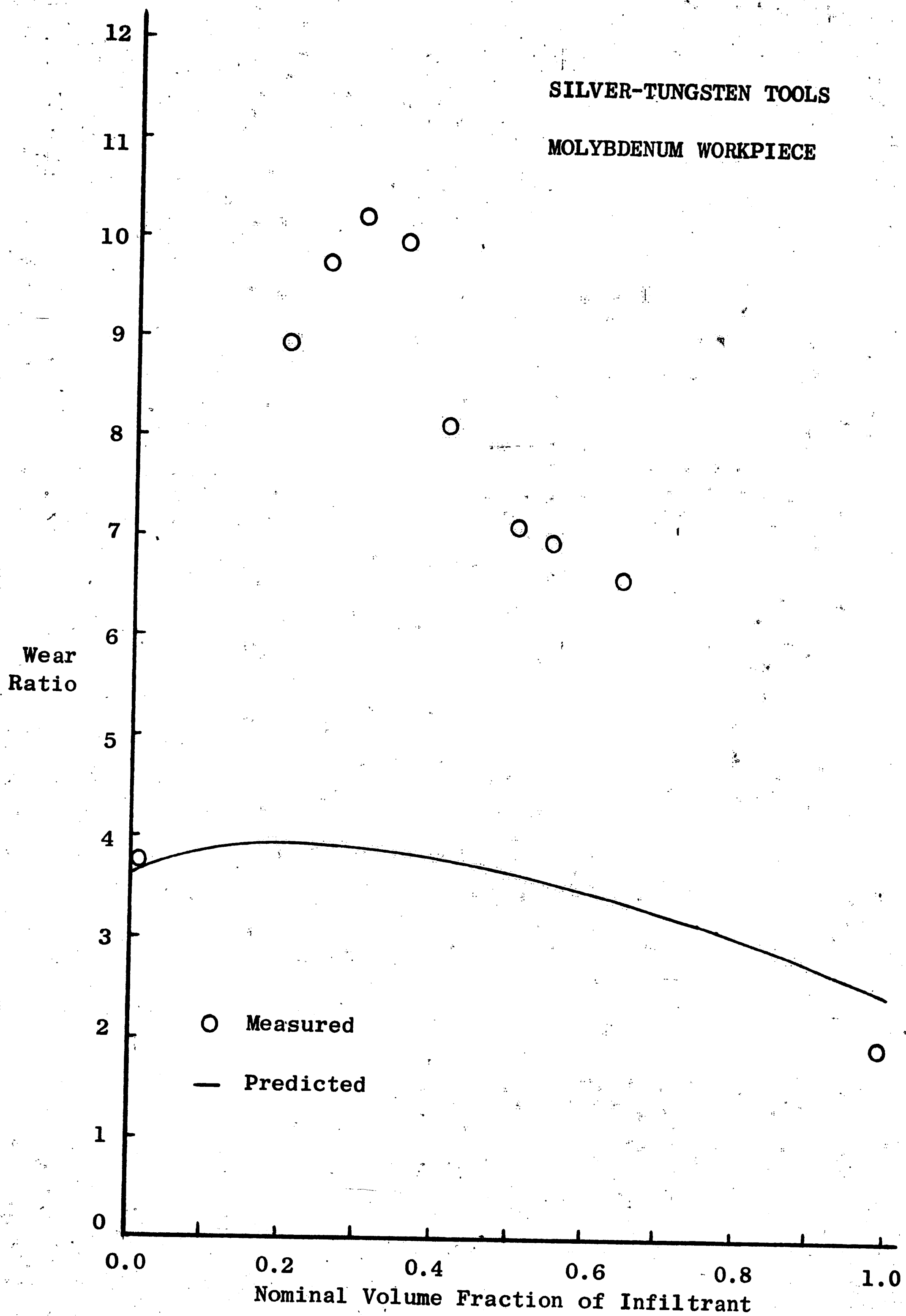
FIGURE 5.   Volumetric Wear Ratio Versus Volume Fraction of
Silver Infiltrant (Silver-Tungsten Composite
Tools, Molybdenum Workpiece)
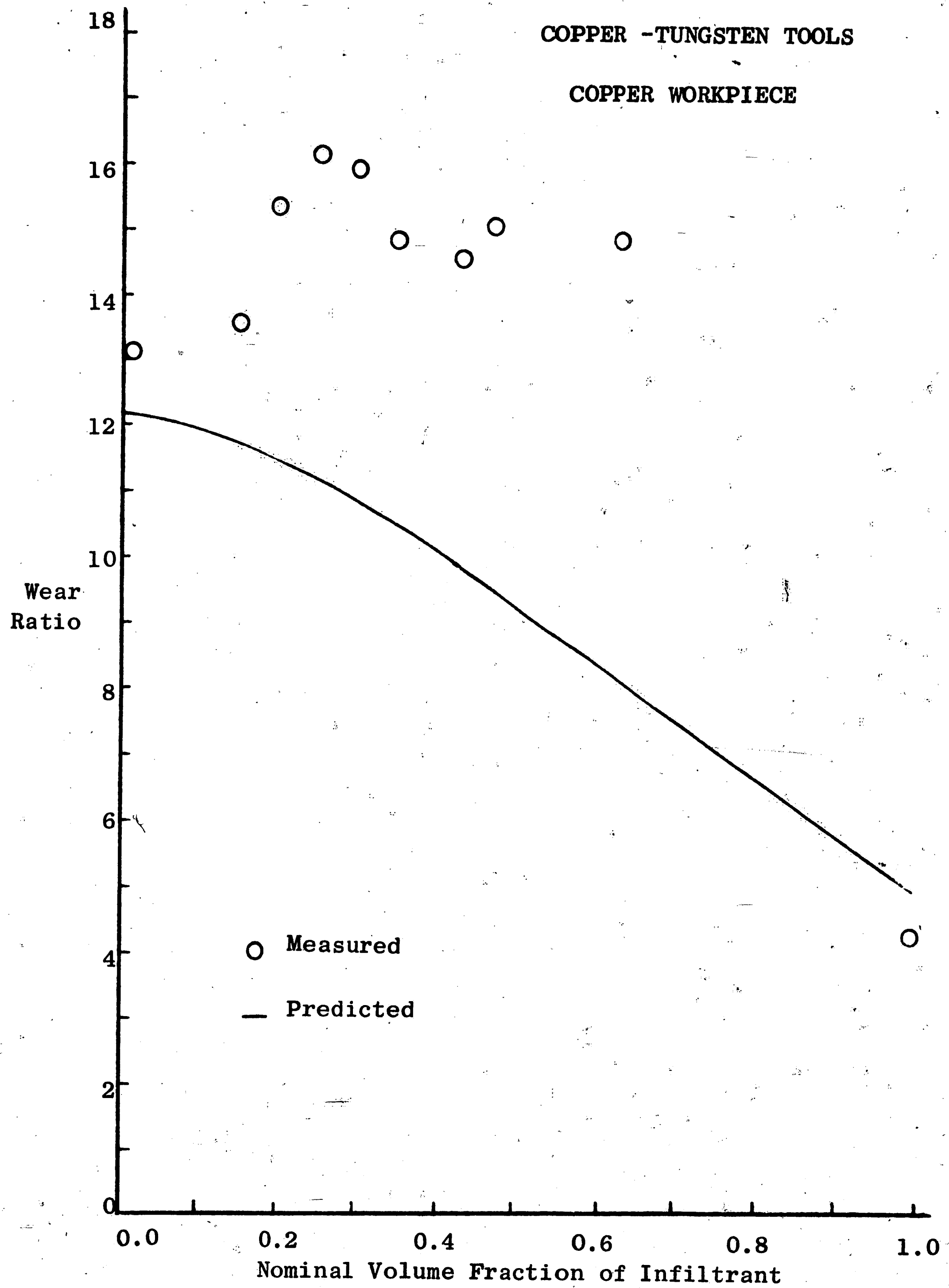
FIGURE 6. Volumetric Wear Ratio Versus Volume Fraction of
Copper Infiltrant (Copper-Tungsten Composite
Tools, Copper Workpiece)
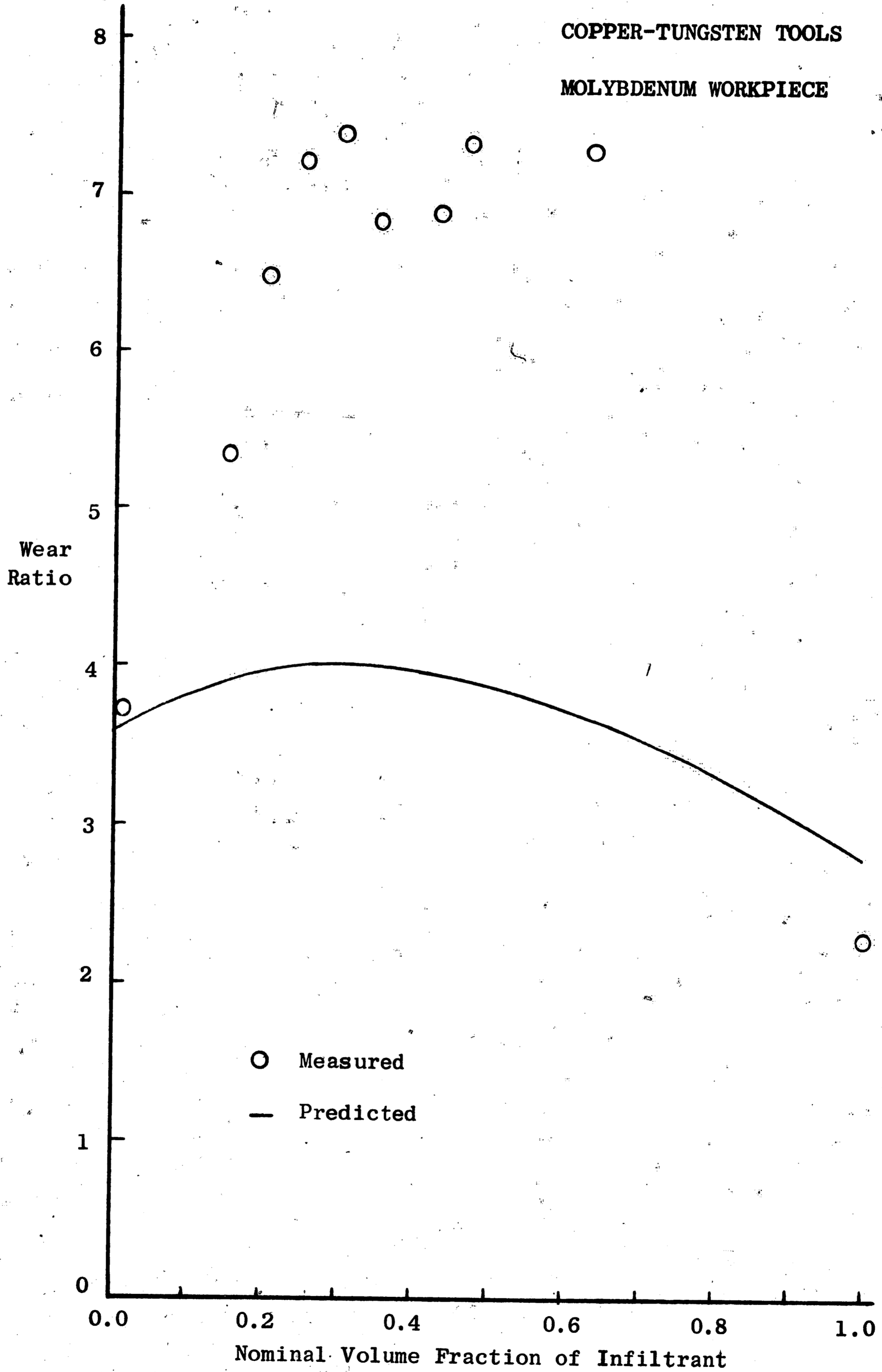
FIGURE 7. Volumetric Wear Ratio Versus Volume Fraction of Copper Infiltrant (Copper-Tungsten Composite Tools, Molybdenum Workpiece)
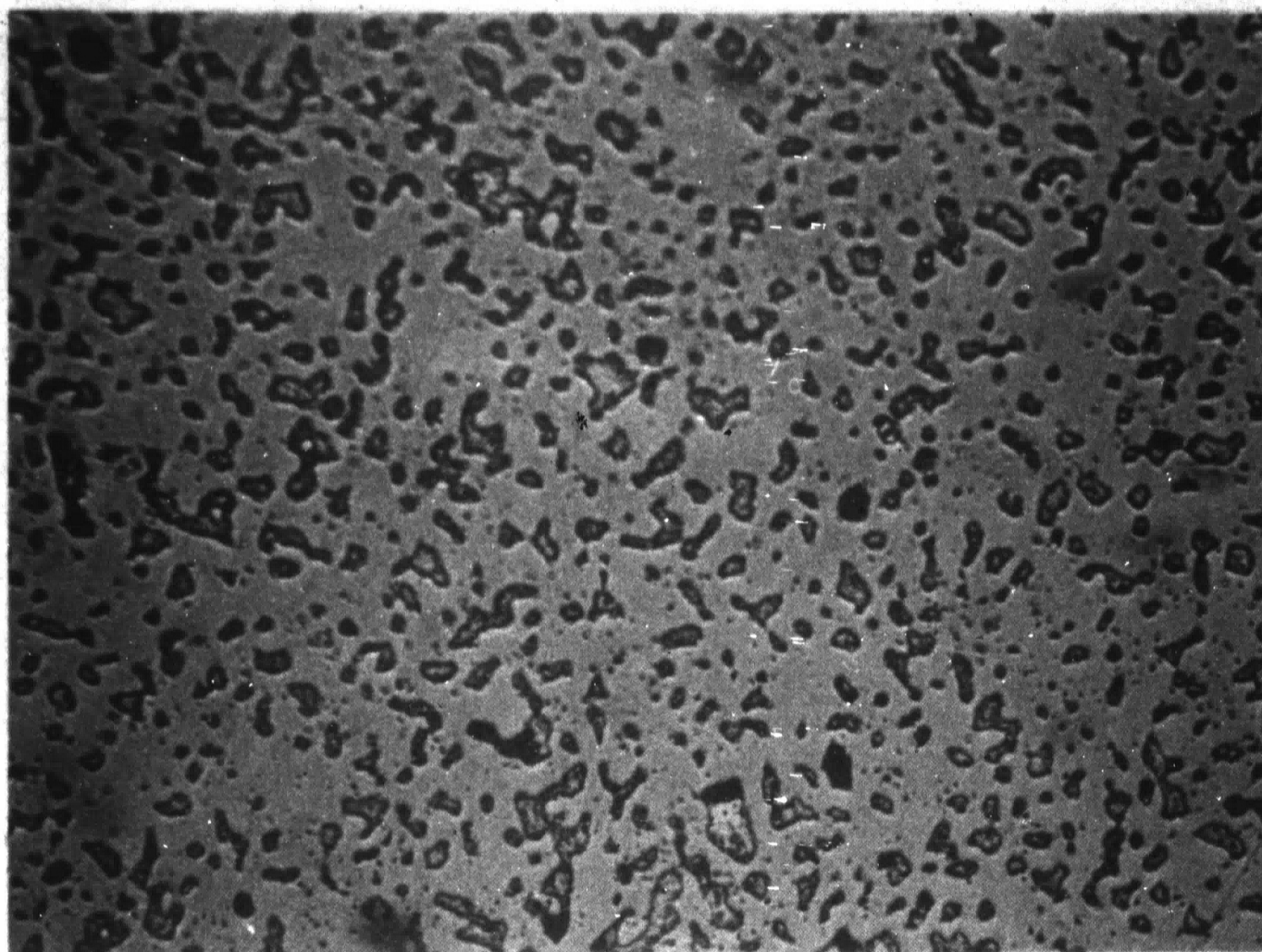
FIGURE 8.   Photomicrograph of 20 Ag-80W
(Nominal Volume Percent),
Unetched (500x), Dark Phase
Ag
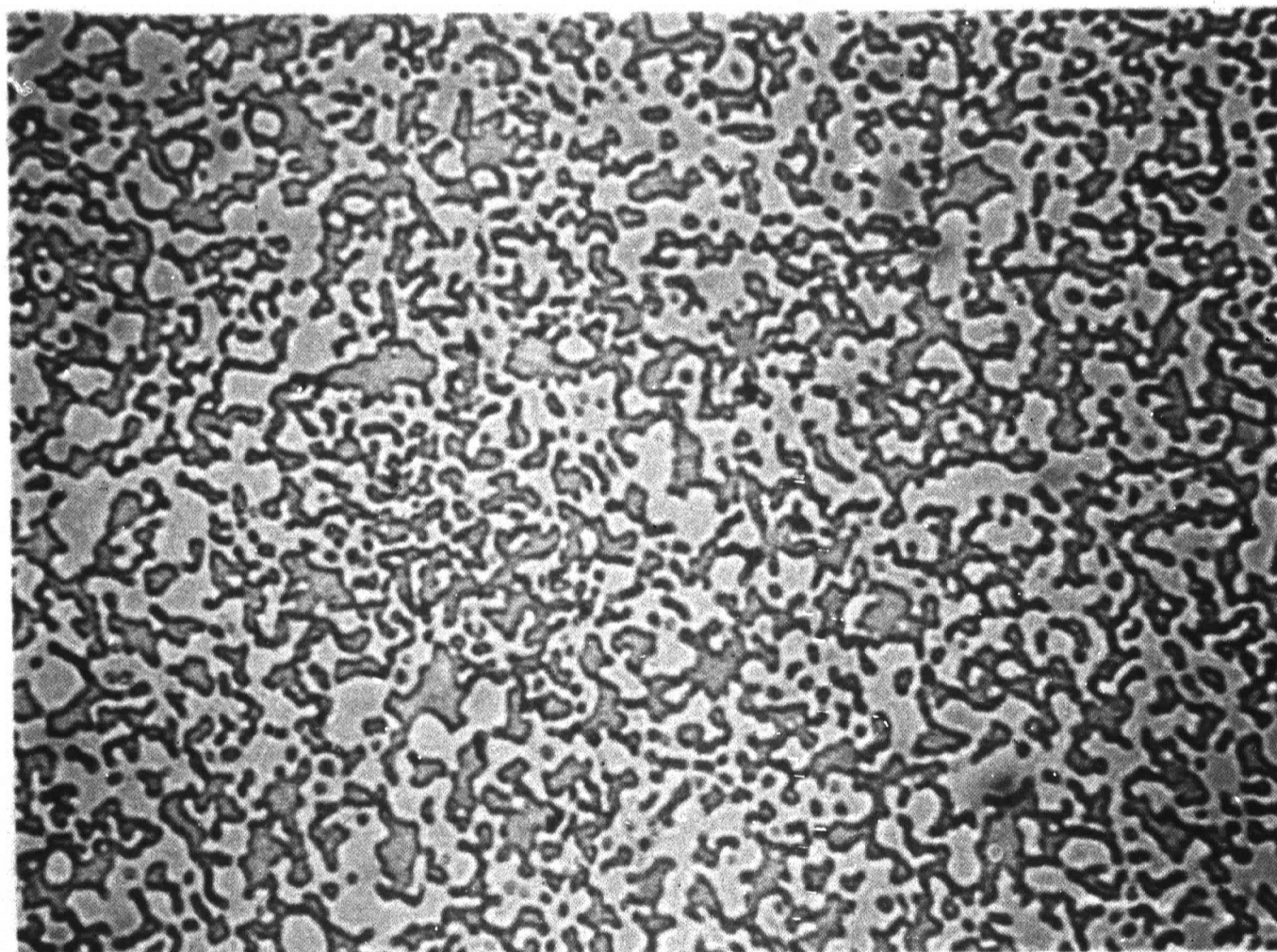
FIGURE 9.   Photomicrograph of 30 Ag-70W
(Nominal Volume Percent),
Unetched (500x), Dark Phase
Ag
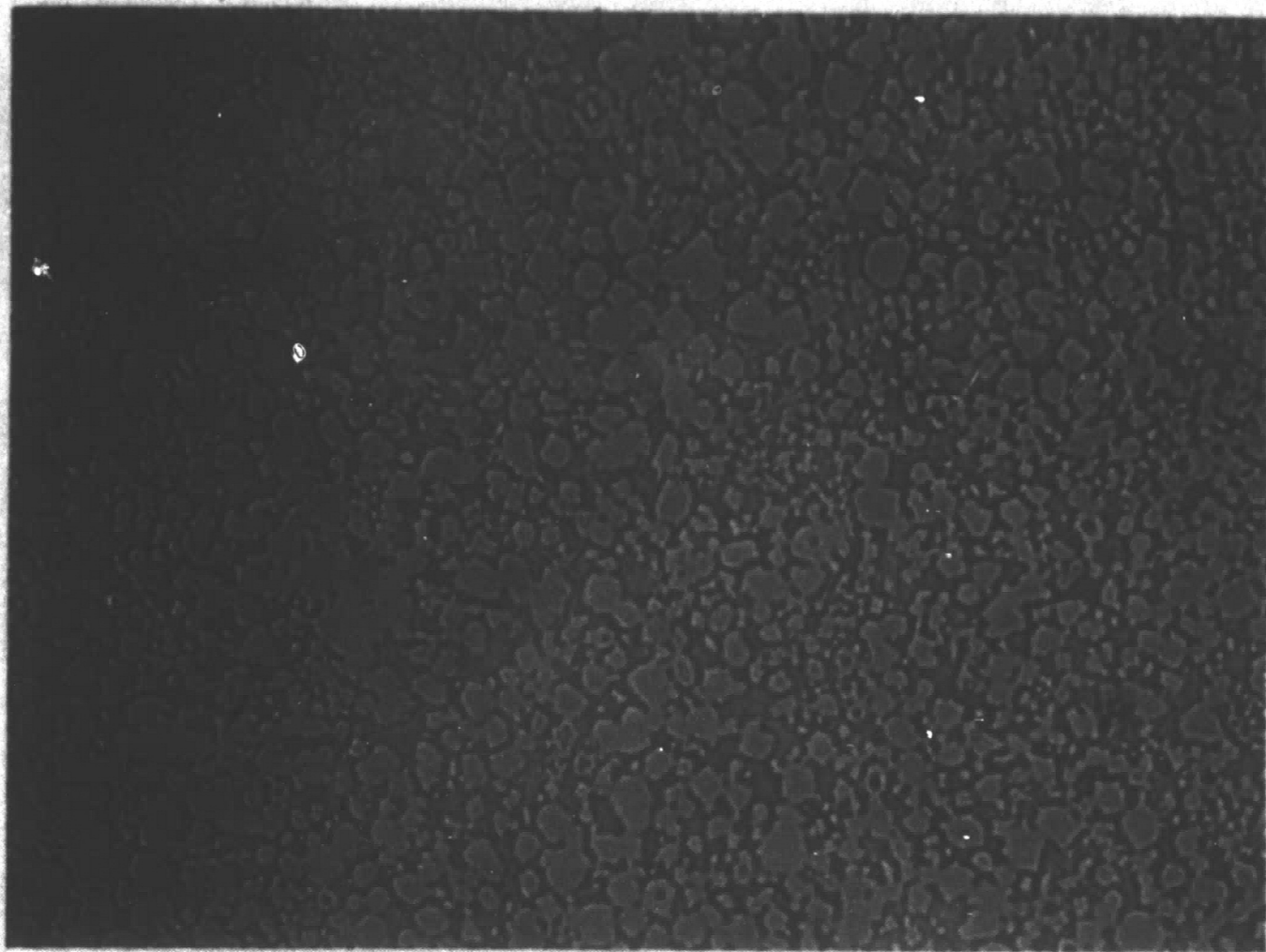
FIGURE 10. Photomicrograph of 41 Ag-59 W
(Nominal Volume Percent), Un-
etched (500x), Dark Phase Ag
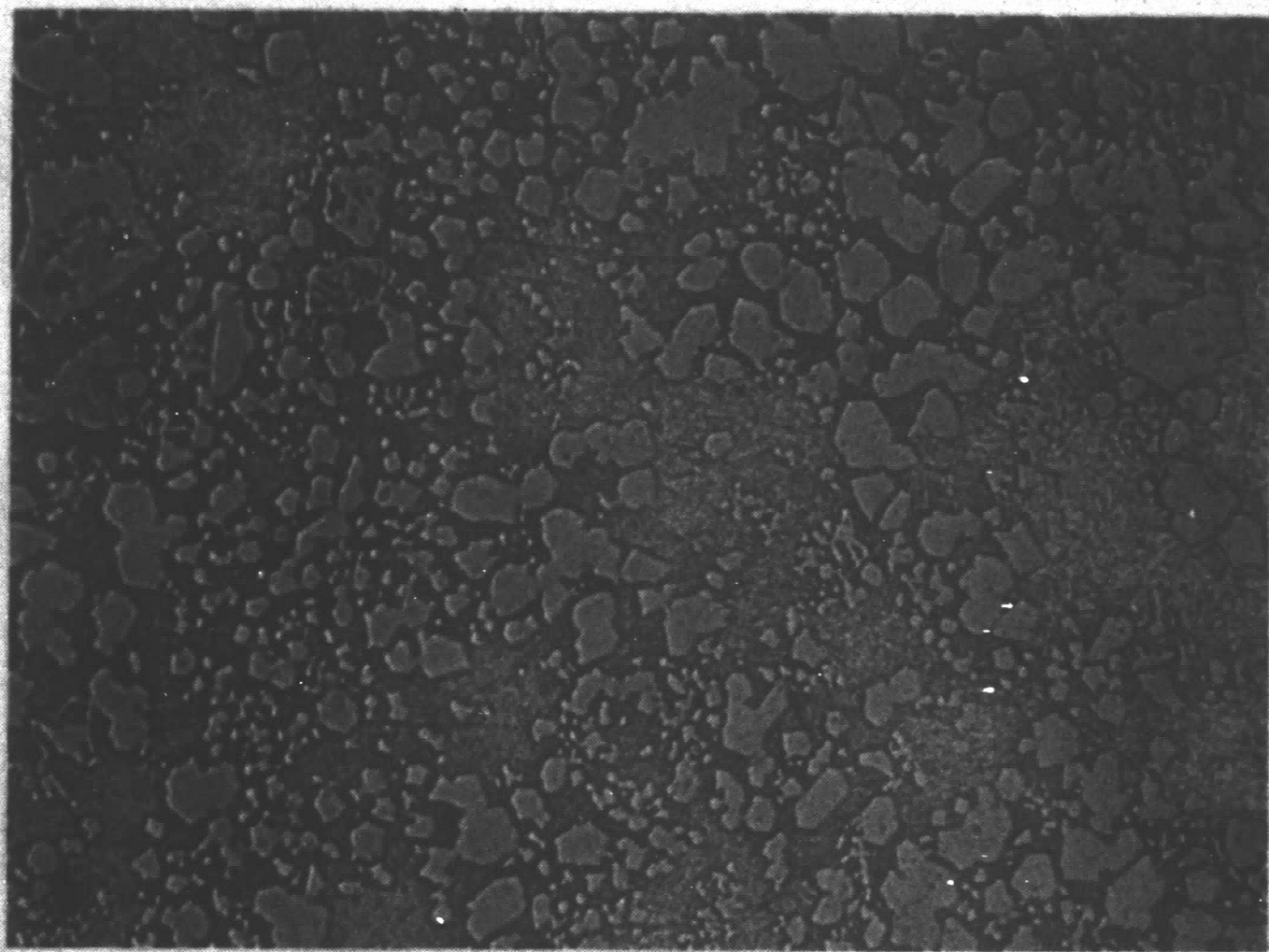
FIGURE 11. Photomicrograph of 50 Ag-50W
(Nominal Volume Percent), Un-
etched (500x), Dark Phase Ag
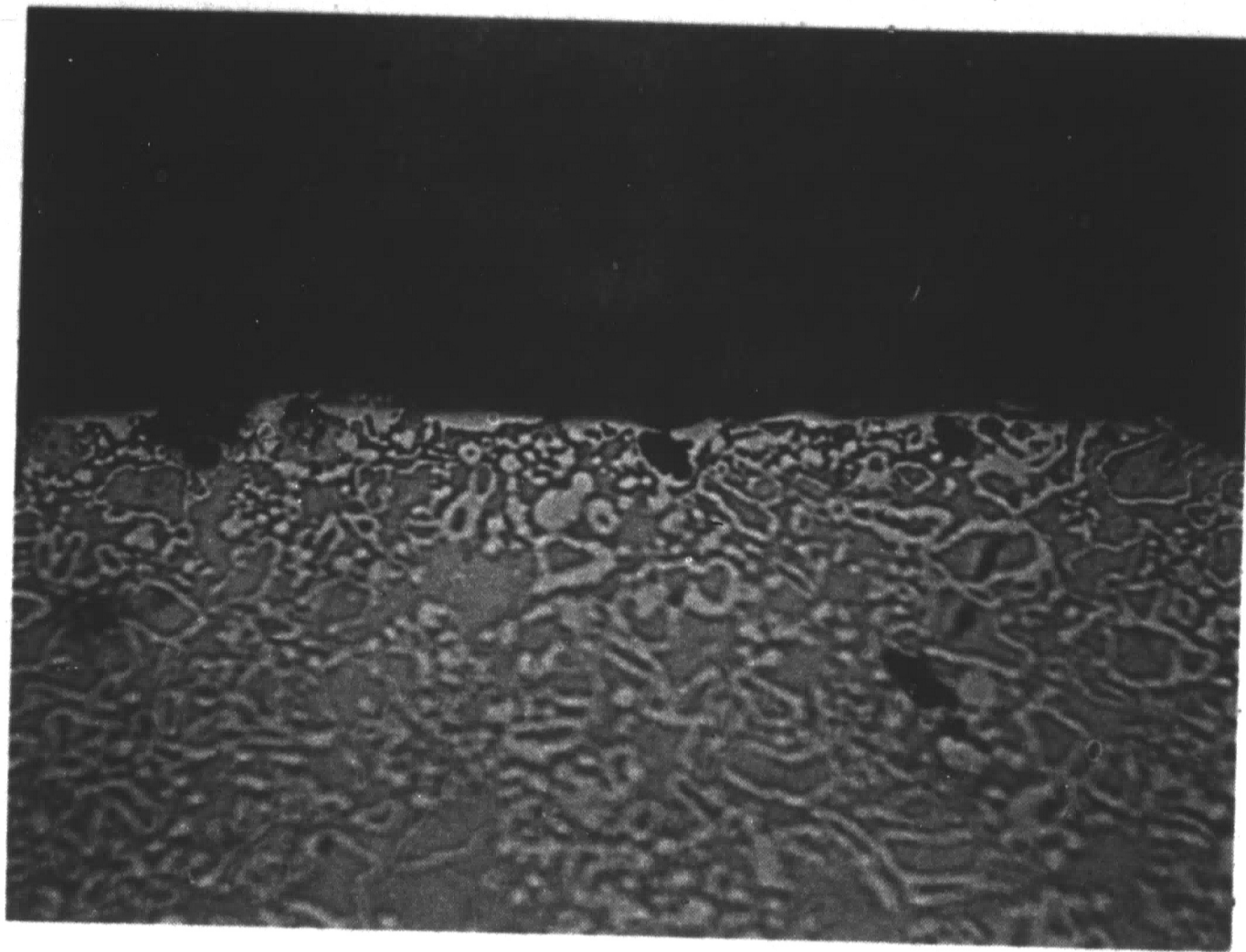
FIGURE 12.   Photomicrograph of Cross-Section of Machined Surface of 63 Cu-37W (Nominal Volume Fraction) Tool Showing a Thin, Fairly Continuous Layer of Tungsten on Machined Surface (Unetched, 500x), Dark Phase Cu
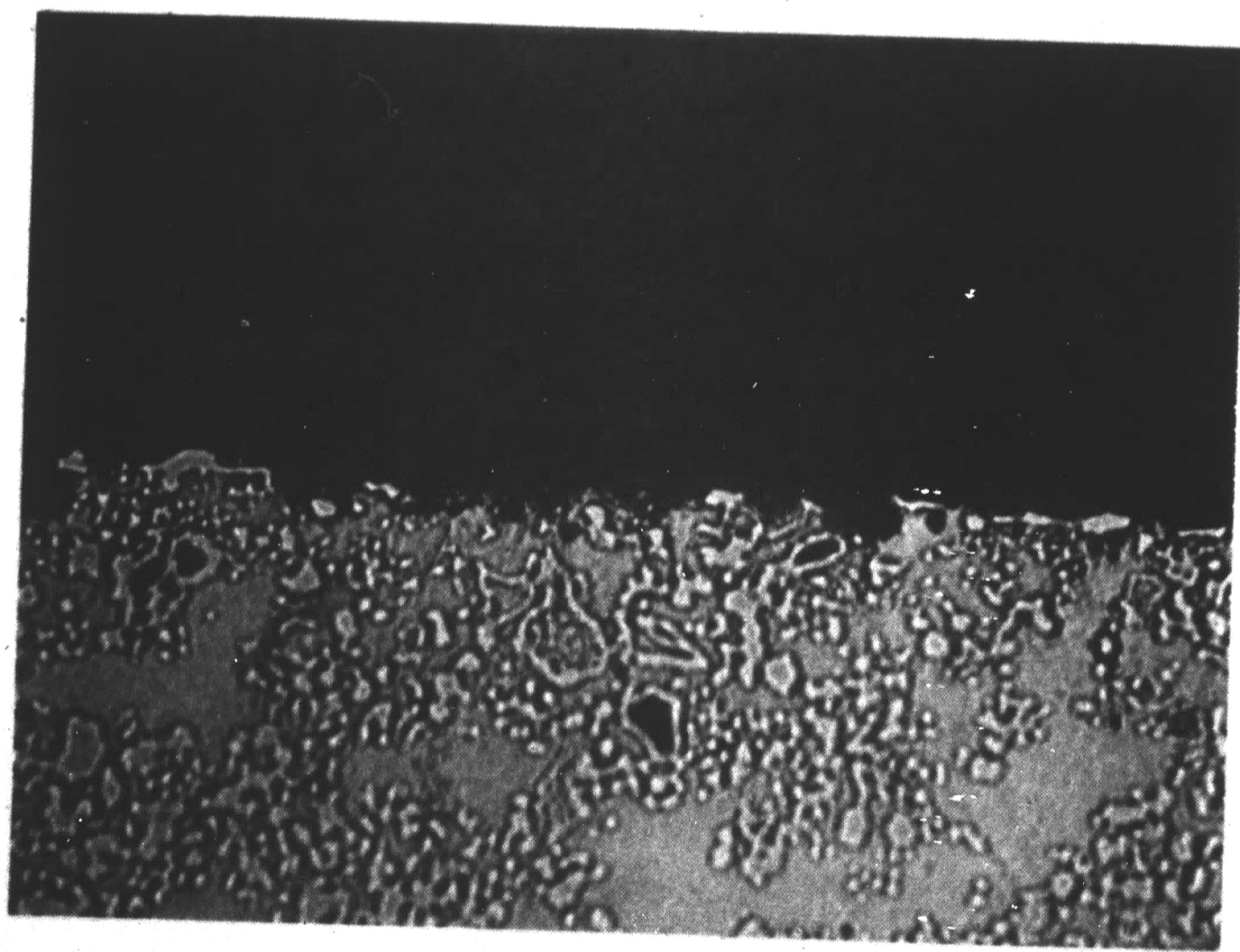
FIGURE 13.   Photomicrograph of Cross-Section of Machined Surface of a 64 Ag-36W (Nominal Volume Percent) Tool, Note Absence of Thin Layer of Tungsten on Machined Surface (Unetched, 500x), Dark Phase Ag
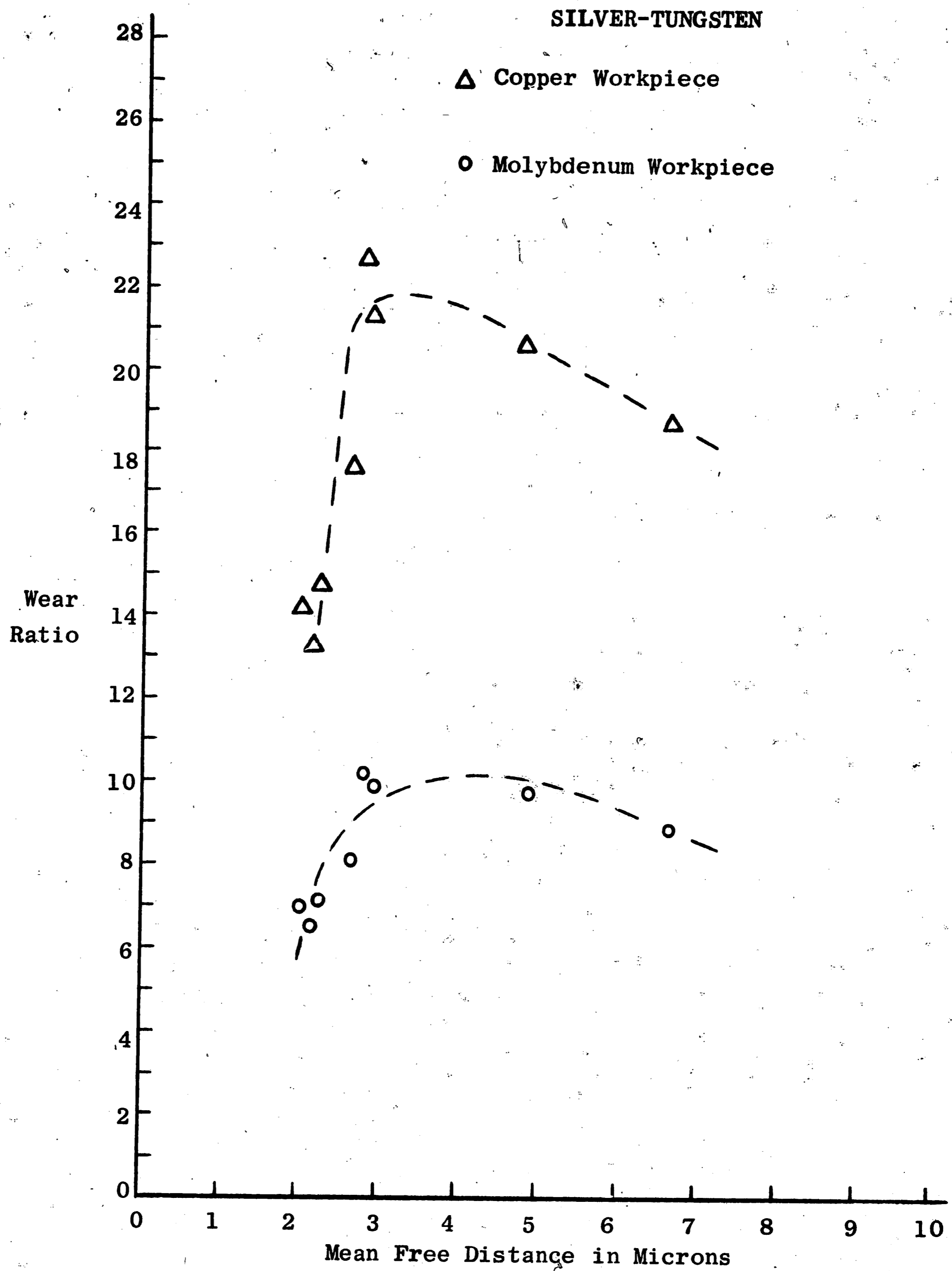
FIGURE 14. Volumetric Wear Ratio Versus Mean Free Distance
(Surface to Surface) Between Silver Infiltrant
"Particles" in Silver-Tungsten Composites
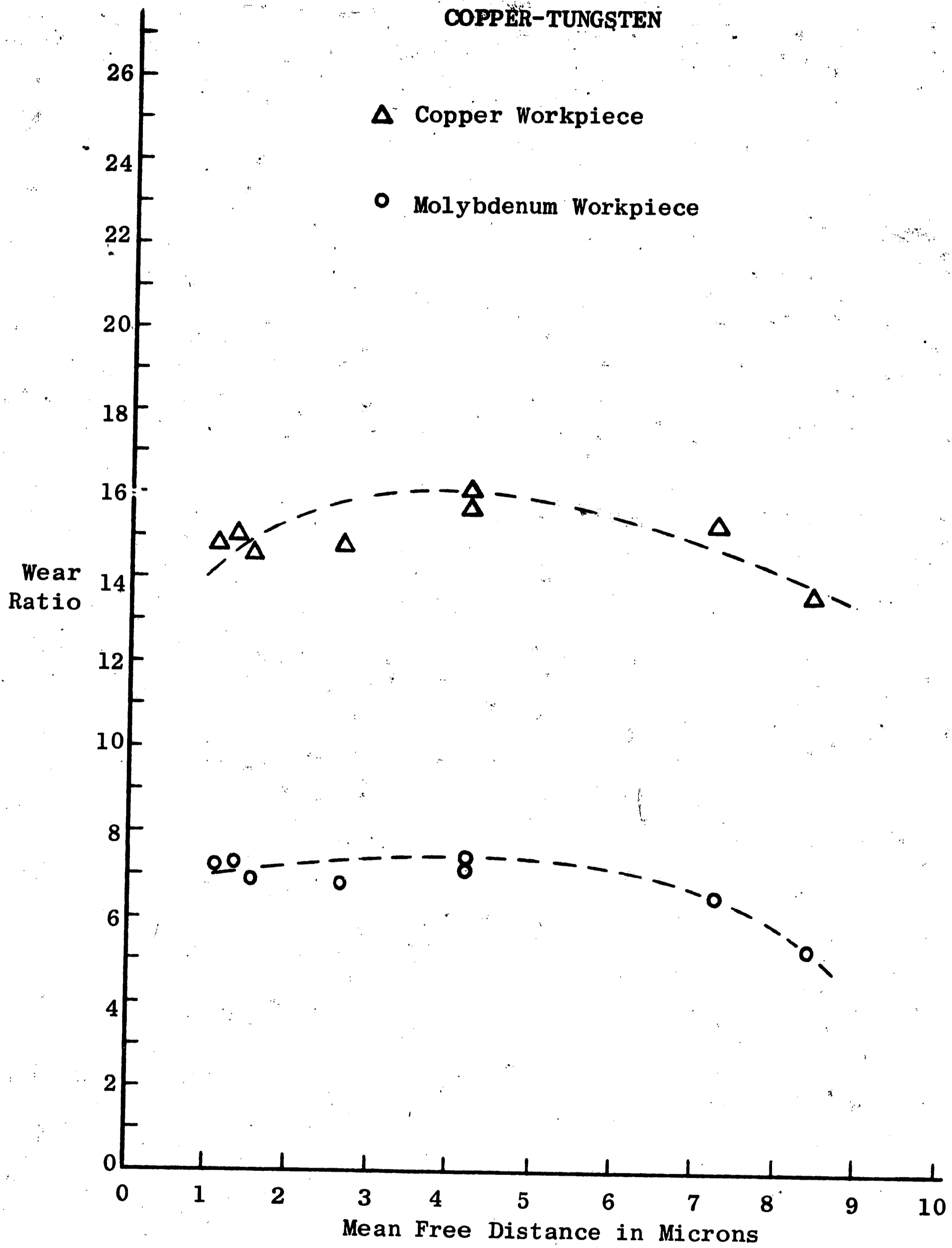
FIGURE 15. Volumetric Wear Ratio Versus Mean Free Distance (Surface to Surface) Between Copper Infiltrant "Particles" in Copper-Tungsten Composites
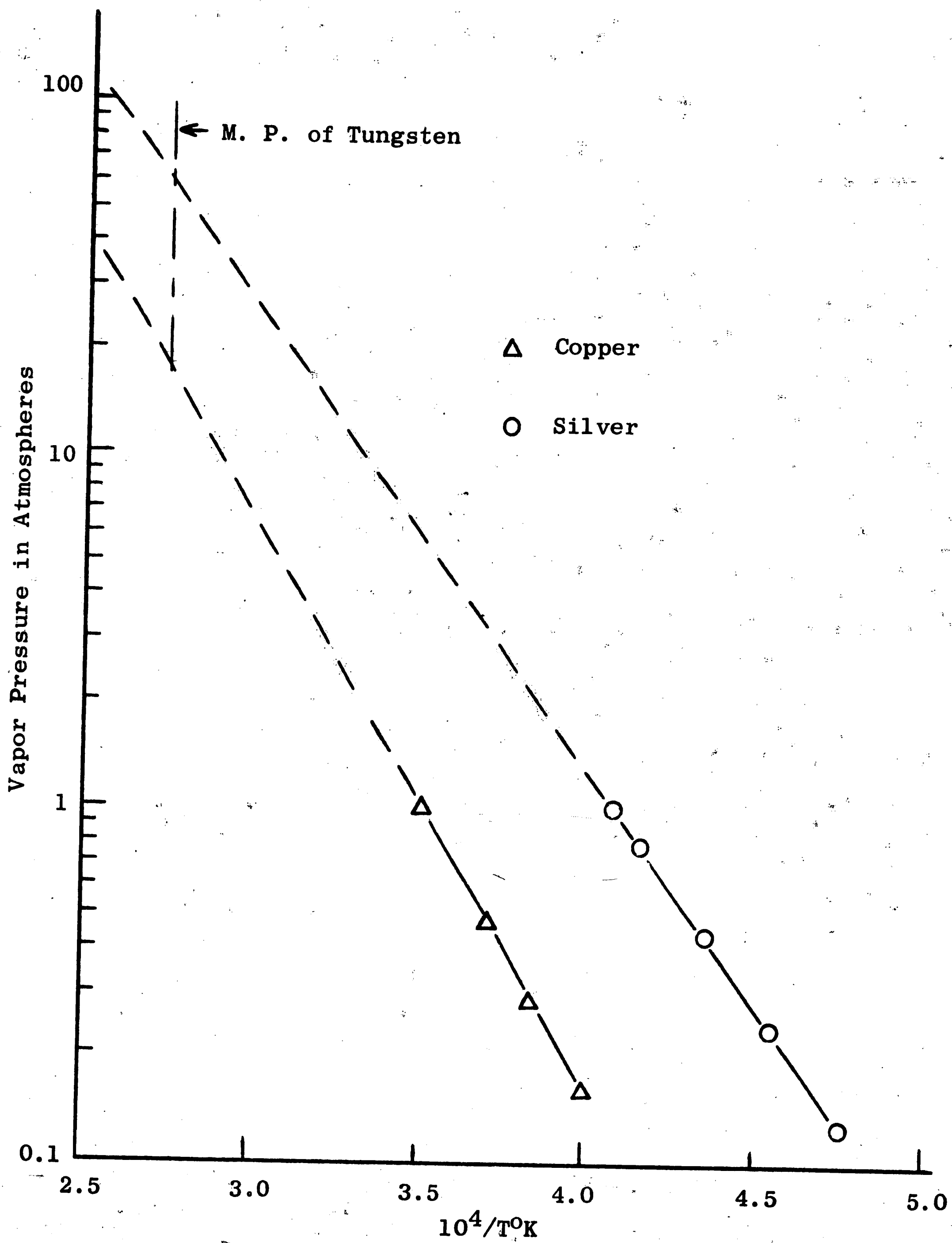
FIGURE 16.   Extrapolated Vapor Pressure of Copper and Silver
(Obtained From Reference 24)

TABLE I

Properties of Composite Materials

Material	Obtained From Quantitative Metallography			
Nominal Volume Percent of Infiltrant in Tungsten Matrix**	Volume Percent Infiltrant	Volume Percent Voids	Interfacial Intercepts per mm	Mean Free Distance Between Infiltrant "Particles" in Microns
20% Ag	13.3	1.8	120	6.65
25% Ag	17.6	1.1	156	4.80
30% Ag	29.7	0.4	250	2.80
35% Ag	30.2	1.1	225	2.89
41% Ag	35.4	1.4	222	2.66
50% Ag	43.4	2.9	224	2.23
55% Ag	43.6	2.8	223	2.02
64% Ag	57.5	4.7	167	2.16
15% Cu	12.2	2.1	101	8.40
20% Cu	14.9	1.3	110	7.27
25% Cu	22.3	2.6	179	4.19
30% Cu	24.7	2.4	164	4.21
35% Cu	27.6	0.7	246	2.64
43% Cu	28.2	2.9	370	1.54
47% Cu	50.9	1.4	398	1.33
63% Cu	54.2	3.5	338	1.09

TABLE I (cont'd)

Material	Measured		Calculated*	
Nominal Volume Percent of Infiltrant in Tungsten Matrix**	Density gm/cm^3	Electrical Conductivity (microhm-cm)$^{-1}$	Effective Cohesive Energy Kcal/mole @ 298°K	Electrical Conductivity (microhm-cm)$^{-1}$
20% Ag	17.30	0.213	176.1	0.267
25% Ag	16.66	0.237	169.3	0.290
30% Ag	16.57	0.253	162.6	0.313
35% Ag	16.12	0.231	155.9	0.335
41% Ag	15.84	0.300	147.1	0.362
50% Ag	14.33	0.367	135.7	0.403
55% Ag	14.24	0.361	129.0	0.426
64% Ag	13.26	0.420	110.8	0.466
15% Cu	17.52	0.183	187.4	0.240
20% Cu	17.11	0.180	178.6	0.261
25% Cu	16.52	0.182	172.5	0.282
30% Cu	15.91	0.178	166.4	0.303
35% Cu	15.39	0.196	160.3	0.324
43% Cu	14.74	0.255	149.4	0.358
47% Cu	14.16	0.288	146.9	0.376
63% Cu	12.65	0.358	125.0	0.442

*Calculated from the assumption that in non-alloying binary composites, the cohesive energy and electrical conductivity are theoretically (according to the rule of mixed proportions) linear functions of the composition (given in volume percent).

**Obtained from the Mallory Matallurgical Co., Indianapolis, Indiana.

TABLE II

Properties of Elemental Materials*

Element	Density gm/cm^3	Melting Point ^{o}C	Boiling Point ^{o}C	Electrical Conductivity (microhm-cm)$^{-1}$	Cohesive Energy K cal/mole @ 298°K
Silver	10.49	960.8	2210	.629	68.4
Copper	8.96	1083.0	2595	.598	81.1
Tungsten	19.3	3410	5930	.177	203
Molybdenum	10.22	2610	5560	.192	157.5

*Obtained from Reference 25.

TABLE III

Averaged Values of Volumetric Wear Ratio Data

Tool Composite (Volume Percent Infiltrant in Tungsten Matrix)	Workpiece	
	Copper	Molybdenum
20% Ag	18.68	8.90
25% Ag	20.58	9.73
30% Ag	22.68	10.22
35% Ag	21.28	9.95
41% Ag	17.58	8.11
50% Ag	14.73	7.12
55% Ag	14.17	6.95
64% Ag	13.28	6.53
15% Cu	13.57	5.32
20% Cu	15.32	6.47
25% Cu	16.12	7.19
30% Cu	15.87	7.37
35% Cu	14.79	6.82
43% Cu	14.57	6.86
47% Cu	15.01	7.31
63% Cu	14.80	7.26

Elemental

	Copper	Molybdenum
Cu	4.24	2.28
Ag	4.31	1.95
W	13.14	3.72

TABLE IV

Individual Test Values of Volumetric Wear Ratio

Tool	Workpiece					
Composite (Volume Percent Infiltrant in Tungsten Matrix)	Copper			Molybdenum		
	W_t	W_w	WR	W_t	W_w	WR
20% Ag	5.1	52.3	19.872	7.8	37.9	8.230
	4.3	44.5	20.054	6.3	34.1	9.167
	3.6	39.4	20.345	5.3	26.6	8.500
	4.9	38.8	15.344	5.1	27.1	8.999
	4.0	36.7	17.779	4.4	24.9	9.585
25% Ag	5.0	53.1	19.741	6.0	37.1	10.046
	4.2	45.5	20.138	5.4	34.0	10.230
	3.6	39.4	20.345	4.6	27.2	9.607
	3.6	39.6	20.448	4.5	27.2	9.820
	3.4	35.7	19.518	5.7	26.2	7.468
	3.7	37.5	18.840	4.8	30.2	10.222
	3.6	43.1	22.255	3.9	24.7	10.290
	4.1	51.6	23.395	4.4	27.5	10.154
30% Ag	3.4	36.6	19.996	4.5	28.9	10.427
	3.9	48.0	22.861	4.5	28.6	10.318
	3.6	48.8	25.180	4.6	28.1	9.918
35% Ag	3.8	41.2	19.590	4.1	26.2	10.092
	3.8	44.8	21.302	4.6	23.9	10.059
	4.1	52.1	22.961	4.8	29.5	9.705
41% Ag	5.2	49.8	17.001	6.2	33.2	8.308
	4.3	42.9	17.710	6.6	34.7	8.157
	3.8	37.6	17.565	5.1	25.6	7.788
	3.8	37.7	17.611	4.8	24.9	8.048
	3.6	36.5	17.998	4.6	24.5	8.264
50% Ag	5.3	44.3	13.424	6.3	32.2	7.174
	4.4	42.0	15.330	8.5	43.7	7.216
	4.0	38.0	15.257	5.2	25.3	6.830
	3.9	36.4	14.989	4.8	26.4	7.194
	3.9	35.6	14.660	4.7	24.0	7.168

TABLE IV (cont.)

Individual Test Values of Volumetric Wear Ratio

Tool						
	Workpiece					
Composite (Volume Percent Infiltrant in Tungsten Matrix)	Copper			Molybdenum		
	W_t	W_w	WR	W_t	W_w	WR
55% Ag	4.1	35.2	13.707	4.8	23.4	6.802
	4.8	41.5	13.803	5.1	25.8	7.059
	4.5	42.3	15.007	5.2	26.0	6.977
64% Ag	5.4	48.6	13.379	6.3	32.2	7.129
	4.3	40.9	14.140	9.6	48.1	6.510
	4.2	34.0	12.034	5.3	25.3	6.202
	4.1	36.2	13.125	4.9	24.0	6.364
	3.6	33.2	13.709	4.8	23.8	6.442
15% Cu	6.6	45.8	13.625	9.0	27.1	5.167
	5.0	34.6	13.587	9.3	29.3	5.407
	5.1	35.8	13.783	7.2	22.4	5.339
	5.2	35.2	13.291	7.4	22.6	5.241
				6.4	20.3	5.443
20% Cu	4.3	32.7	14.583	6.1	24.0	6.594
	5.3	42.2	15.269	8.2	31.7	6.479
	5.2	43.7	16.115	7.5	28.4	6.347
25% Cu	3.1	26.3	15.712	5.6	25.4	7.342
	4.8	41.3	15.934	6.4	28.2	7.132
	4.8	43.3	16.706	6.1	28.6	7.111
30% Cu	5.6	48.5	15.445	6.9	32.7	7.387
	5.3	46.6	15.680	7.0	33.1	7.370
	4.1	36.9	16.050	5.4	24.8	7.158
	4.2	37.3	15.838	5.3	25.1	7.382
	3.7	31.2	15.038	5.3	25.3	7.440
	3.7	33.3	16.050	5.4	25.8	7.447
	4.5	40.8	16.169	5.5	26.2	7.425
	4.5	42.2	16.724	5.6	26.3	7.320
35% Cu	4.1	33.0	13.888	5.2	23.9	6.932
	4.9	42.5	14.966	5.7	26.2	6.932
	4.7	42.3	15.530	5.9	25.8	6.595

TABLE IV (cont.)

Individual Test Values of Volumetric Wear Ratio

Tool		Workpiece				
Composite (Volume Percent Infiltrant in Tungsten Matrix)		Copper			Molybdenum		
	W_t	W_w	WR	W_t	W_w	WR
43% Cu	5.3	47.5	14.807	7.0	33.0	6.807
	5.4	47.6	14.563	6.8	32.7	6.944
	4.1	36.6	14.748	5.2	24.5	6.803
	4.2	37.0	14.554	5.2	24.8	6.887
	3.7	31.8	14.199	-	-	-
47% Cu	5.1	47.5	14.783	6.1	31.7	7.209
	5.0	46.4	14.729	6.1	32.8	7.459
	3.9	37.1	15.099	4.7	24.5	7.231
	4.9	38.8	15.344	4.9	24.9	7.049
	3.8	32.6	15.120	4.7	25.1	7.604
63% Cu	4.6	47.6	14.669	5.3	31.7	7.411
	4.6	46.7	14.392	5.4	31.9	7.319
	3.7	37.4	14.329	4.2	24.9	7.346
	3.5	37.0	14.986	4.4	24.8	6.984
	3.4	33.1	15.641	4.2	24.5	7.228
Elemental						
Cu	6.9	29.4	4.261	7.3	19.0	2.275
	7.2	30.4	4.222	7.5	19.6	2.284
Ag	9.0	33.2	4.333	8.4	16.2	1.980
	9.1	33.2	4.286	10.6	19.9	1.982
W	5.2	31.8	13.159	10.0	20.2	3.761
	5.1	31.1	13.126	10.4	20.4	3.689

W_t = change in weight of tool in milligrams.

W_w = change in weight of workpiece in milligrams.

WR = volumetric wear ratio.

TABLE V

Data from Longfellow's Work[*]

Tool Material	Average Volumetric Wear Ratio		Physical Properties of Tool	
	Copper Workpiece	Molybdenum Workpiece	Cohesive Energy Kcal/mole	Electrical Resistivity microhm-cm
Cadmium	0.1963	0.0666	26.75	6.83
Zinc	0.3123	0.1372	31.2	5.916
Silver	4.6771	2.2946	68.4	1.59
Copper	4.7849	2.6434	81.1	1.6730
Gold	2.8417	1.7477	87.3	2.35
Cobalt	1.0916	0.3347	101.6	6.24
Nickel	1.0585	0.3118	102.8	6.84
Molybdenum	5.2084	1.6425	157.5	5.2
Tungsten	12.900	3.9132	203	5.65

[*]Data was obtained from Reference 7

48

REFERENCES

1. Lloyd, H. K. and R. H. Warren, "Metallurgy of Spark-Machined Surfaces," Journal of the Iron and Steel Institute (3), Vol. 203 (1965), pp. 238-247.

2. Lazarenko, B. R., "Physical Principles of Electric-Spark Metal-Working," Vestnik Akademii nauk SSSR (6), Vol. 29 (1959), pp. 49-56. Translated by Translation Services Branch, Foreign Technology Division, Wright-Patterson Air Force Base, Ohio.

3. Gaus, A. R., "Pick the Right EDM Electrode," American Machinist/ Metalworking Manufacturing (7), Vol. 105 (1961), p. 90.

4. Bibliography of Electric Discharge Machining, 6th ed., Warren, Michigan: General Motors Corporation, 1963.

5. Hill, D. H., "Electrical Discharge Machining," Metals Engineering Quarterly (3), Vol. 2 (1962), pp. 22-27.

6. Nekrashevic, I. G. and I. A. Bakuto, "Present State of the Theoretical Concepts of the Electric Erosion of Metals," Electrospark Machining of Metals (Vol. 3), B. A. Krasyuk, editor. Translated from Russian. New York: Consultant's Bureau Enterprises, Inc., 1965.

7. Longfellow, J., "The Effects of Electrode Material Properties on the Wear Ratio in Spark Machining." Unpublished Master's Thesis, Lehigh University, 1966.

8. Berghausen, P. E., H. D. Brettschneider, F. M. Davis et al., Electro-Discharge Machining Program, Cincinnati Milling and Grinding Machines, Inc. Final Technical Documentary Report No. ASD-TDR-T-545 (1963), Advanced Fabrication Techniques Branch (MATF), Manufacturing Technology Division, Air Force Materials Laboratory, Air Force Systems Command, Wright-Patterson Air Force Base, Ohio.

9. Zingerman, A. S., "Mechanism of Electrical Erosion," Izvestiya Vysshikh Uchebnykh Zavedeniy Fizika (1), (1963), pp. 21-30. Translated by Translation Services Branch, Foreign Technology Division, Wright-Patterson Air Force Base, Ohio.

10. Jones, F. L., "Electrode Erosion by Spark Machining," British Journal of Applied Physics (3), Vol. 1 (1950), pp. 61-65.

REFERENCES (cont.)

11. Williams, E. M. and R. E. Smith, "Phenomena Accompanying Transient Low Voltage Discharges in Liquid Dielectrics," _Trans. A.I.E.E._ (1), Vol. 76 (1957), pp. 93-97.

12. Price, E., "A Metallurgical Approach to Electrical Discharge Machining Phenomena." Unpublished Master's Thesis, Lehigh University, 1965.

13. Park, J. H., "Shunts and Inductors for Surge-Current Measurements," _Journal of Research of the National Bureau of Standards_, Vol. 39 (1947), pp. 191-212.

14. Rostoker, W. and J. R. Dvorak, _Interpretation of Metallographic Structures_, New York: Academic Press, 1965.

15. Underwood, E. E., "Quantitative Metallography," _Metals Engineering Quarterly_ (3), Vol. 1 (1961), pp. 70-81.

16. Gurland, J., "The Measurement of Distribution, Spacing, Contact and Continuity of Particles in a Matrix," _Plansee Siminar_, (1961), pp. 507-518.

17. Naidich, Yu. V., I. A. Lavrineko, and V. N. Eremenko, "Capillary Phenomena in the Densification Process During Sintering in the Presence of the Liquid Phase," _International Journal of Powder Metallurgy_ (4), Vol. 1 (1965), pp. 41-48.

18. Meyer, G. E., "The Role of Powder Metallurgy in Manufacture of Electric Contacts," _Metal Progress_ (6), Vol. 87 (1965), pp. 95-99.

19. Matt, R. E. and J. J. Warga, "Development of Silver Infiltrated Tungsten Nozzles for Uncooled Rocket Motors," _Plansee Siminar_ (5th), (1965), pp. 233-255.

20. Underwood, E. E., "Quantitative Metallography, Part II," _Metals Engineering Quarterly_, (4), Vol. 1 (1961), pp. 62-71.

21. Kronsbein, J., Buteau, L. J. Jr., and DeHoff, R. T., "Measurement of Topological Parameters for Description of Two-Phase Structures with Special Reference to Sintering," _Transactions of the Metallurgical Society of AIME_, Vol. 233 (1965), pp. 1961-1969.

22. Resnick, R., C. Wurms, R. Steinitz, and E. Mazza, "Cooling of Porous Tungsten Structures by Evaporation of Infiltrated Material," _Metals Engineering Quarterly_ (2), Vol. 3 (1963), pp. 51-59.

REFERENCES (cont.)

23. Martin, E. A., "Experimental Investigation of a High-Energy Density, High Pressure Arc Plasma," *Journal of Applied Physics* (2), Vol. 31 (1960), pp. 255-267.

24. Stull, D. R. and G. C. Sinke, *Thermodynamic Properties of the Elements*, Washington, D. C.: American Chemical Society, 1956.

25. *Metals Handbook*, 8th ed., Metals Park, Ohio: The American Society for Metals, 1964.

VITA

The author was born on September 3, 1934 near Lakeland, Florida, the son of Mr. and Mrs. Clarence E. Keen. He attended public schools near and in Lakeland, Florida, graduating from the Lakeland High School in 1953. He served four years as an Aviation Electronic Technician in the U. S. Coast Guard.

In 1957 he entered the St. Petersburg Jr. College, St. Petersburg, Florida. In 1958 he transferred to the University of Florida from which he received his Bachelor of Electrical Engineering Degree in 1961.

In 1961 he was employed by the Western Electric Company, Winston-Salem, North Carolina, working for the Bell Telephone Laboratories. Since the summer of 1965, he has been a graduate student in the Department of Metallurgy and Materials Science of Lehigh University as a participant in the Western Electric Lehigh Master's Program.

The author is a member of the Institute of Electrical and Electronic Engineers.